Cell Transplantation, Vol. 25, pp. 159–182, 2016
Printed in the USA.

0963-6897/16 $90.00 + .00
DOI: http://dx.doi.org/10.3727/096368915X688010
E-ISSN 1555-3892
www.cognizantcommunication.com

Peripheral Nerve Regeneration Through Hydrogel-Enriched Chitosan Conduits Containing Engineered Schwann Cells for Drug Delivery

Cora Meyer,*†[1] Sandra Wrobel,*†[1] Stefania Raimondo,‡ Shimon Rochkind,§ Claudia Heimann,¶ Abraham Shahar,# Ofra Ziv-Polat,# Stefano Geuna,‡ Claudia Grothe,*† and Kirsten Haastert-Talini*†

*Institute of Neuroanatomy, Hannover Medical School, Hannover, Lower-Saxony, Germany
†Center for Systems Neuroscience (ZSN) Hannover, Lower-Saxony, Germany
‡Department of Clinical and Biological Sciences, Università degli studi di Torino, Orbassano, Piemonte, Italy
§Division of Peripheral Nerve Reconstruction, Department of Neurosurgery, Tel Aviv Sourasky Medical Center, Tel Aviv University, Tel Aviv, Israel
¶Medovent GmbH, Mainz, Rhineland-Palatinate, Germany
#N.V.R Research Ltd., Ness-Ziona, Israel

Critical length nerve defects in the rat sciatic nerve model were reconstructed with chitosan nerve guides filled with Schwann cells (SCs) containing hydrogel. The transplanted SCs were naive or had been genetically modified to overexpress neurotrophic factors, thus providing a cellular neurotrophic factor delivery system. Prior to the assessment in vivo, in vitro studies evaluating the properties of engineered SCs overexpressing glial cell line-derived neurotrophic factor (GDNF) or fibroblast growth factor 2 (FGF-2^{18kDa}) demonstrated their neurite outgrowth inductive bioactivity for sympathetic PC-12 cells as well as for dissociated dorsal root ganglion cell drop cultures. SCs within NVR-hydrogel, which is mainly composed of hyaluronic acid and laminin, were delivered into the lumen of chitosan hollow conduits with a 5% degree of acetylation. The viability and neurotrophic factor production by engineered SCs within NVR-Gel inside the chitosan nerve guides was further demonstrated in vitro. In vivo we studied the outcome of peripheral nerve regeneration after reconstruction of 15-mm nerve gaps with either chitosan/NVR-Gel/SCs composite nerve guides or autologous nerve grafts (ANGs). While ANGs did guarantee for functional sensory and motor regeneration in 100% of the animals, delivery of NVR-Gel into the chitosan nerve guides obviously impaired sufficient axonal outgrowth. This obstacle was overcome to a remarkable extent when the NVR-Gel was enriched with FGF-2^{18kDa} overexpressing SCs.

Key words: Cellular drug delivery system; Schwann cells (SCs); Sciatic nerve regeneration; Fibroblast growth factor-2; Glial cell line-derived neurotrophic factor (GNDF); Chitosan

INTRODUCTION

Lesions to the peripheral nervous system (PNS) following traumatic events like car accidents and sport as well as military injuries (16,59) are annually reported from more than 1 million people worldwide. The degree of regained function is dependent on the severity of the injury. Spontaneous recovery is possible if the continuity of the nerve trunk is preserved, while cases of complete nerve transection require surgical intervention (19). Up until now, autologous nerve grafts (ANGs) remain the gold standard for peripheral nerve reconstruction. Their usage, however, implicates certain disadvantages like donor site morbidity, limited supply of suitable tissue in case of extended plexus injuries, and mismatch issues regarding among others axonal size, distribution, and alignment (16). Despite modern microsurgery techniques, incomplete or incorrect target reinnervation is still unavoidable (14,16,29). In consequence, patients experience deficits in sensory and motor function and neuropathic pain (8,20,21).

Artificial nerve guides of various biodegradable materials have been tested as alternatives to ANGs and are known to provide a regeneration-promoting environment for regrowing axons (38). Nevertheless, clinical usage of FDA- or CE-approved hollow nerve guides is so far limited to bridge nerve defects of up to a maximum length of 3 cm. Furthermore, results after artificial nerve grafting are also variable and often insufficient with regard to functional recovery (9,16,43).

Received July 29, 2014; final acceptance April 8, 2015. Online prepub date: April 14, 2015.
[1]These authors provided equal contribution to this work.
Address correspondence to Kirsten Haastert-Talini, Hannover Medical School, Institute of Neuroanatomy, OE 4140, Carl-Neuberg-Str.1, D-30625 Hannover, Germany. Tel: +49-511-532-2891; Fax: +49-511-532-2880; E-mail: Haastert-talini.kirsten@mh-hannover.de

In order to enhance the rate of successful regeneration across long gaps reconstructed with artificial nerve guides, luminal enrichment with filaments, sponges, or hydrogels containing collagen or laminin has been considered (13,16,17,19). Three-dimensional guidance structures within the conduit may be advantageous to support Schwann cell (SC) migration and axonal outgrowth (13). To further enhance the chance of successful regeneration across long defects, the addition of regeneration-supporting cells, such as SCs, as well as the exogenous administration of neurotrophic factors has been brought into research focus (31,51).

In the current study, we enriched hollow conduits made of chitosan with a fine-tuned 5% degree of acetylation, with NVR-Gel as a luminal filler, and added genetically modified neonatal rat SCs as cellular drug delivery system.

The chitosan conduits used in this study have previously been evaluated in a rat model of 10-mm gap repair, where they demonstrated a support of functional regeneration similar to ANGs for the reconstruction of 10-mm gaps (34). Furthermore, the performance of the chitosan conduits has been investigated in critical gap length repair (15-mm rat sciatic nerve gap), and their usage resulted in a 57% success rate (functional and axonal regeneration) in comparison to complete failure of the classic silicone tube approach (23).

To structure the hollow lumen of the chitosan conduits in the current study, we utilized NVR-Gel, a hydrogel composed mainly of high molecular weight hyaluronic acid (3×10^6 Da) and laminin that has been developed as a regenerative matrix for nerve repair (65). NVR-Gel has already demonstrated valuable properties allowing neurite outgrowth in vitro (53,79).

To additionally deliver regeneration supporting neurotrophic factors with the nerve conduit, we used somatic ex vivo gene transfer to transplanted SCs. Nonvirally transfected neonatal rat SCs overexpressing isoforms of fibroblast growth factor-2 (FGF-2) have already demonstrated specific support of axonal regeneration across 15-mm sciatic nerve gaps, when delivered within Matrigel-filled silicone conduits (32,68). The FGF-2 system is specifically regulated after peripheral nerve injury as it is described that SCs as well as macrophages at the lesion site express FGF-2 isoforms and FGF receptors (26,28). Following nerve transection, the isoforms are differently regulated with an overall increase of all three isoforms in the proximal nerve stump (more pronounced upregulation of FGF-2^{18kDa} and FGF-2^{21kDa} than of FGF-2^{23kDa}) (52). Especially the low molecular weight isoform FGF-2^{18kDa} is upregulated within hours following nerve crush (25) and has been shown to endorse axonal outgrowth in the long gap peripheral nerve regeneration model, and to improve neurite outgrowth of spinal motor neurons (1,2,28).

Another promising candidate for drug delivery of regeneration-promoting proteins is glial cell line-derived neurotrophic factor (GDNF), which is known to act as a survival factor for motor neurons and has a promoting effect on SC proliferation as well as on myelination (11,38,48). GDNF has been shown to be upregulated in SCs at the sciatic nerve transection site peaking at 7 days after lesion (37). Supporting its important role in peripheral nerve regeneration, impaired regeneration following chronic axotomy has been associated with a decline of GDNF expression by chronically denervated SCs (37). In the current study, we suspended naive or genetically engineered SCs in NVR-Gel and injected the suspension as a luminal filler and drug delivery system into hollow chitosan tubes. We proved survival of the SCs within the composite conduits in vitro over a period of 9 days. We further demonstrate that the cells populate the interior NVR-Gel matrix, while demonstrating their typical bipolar morphology. We then reconstructed a defect of 15-mm critical length in the rat sciatic nerve model. Reconstruction conditions and animal groups were set as follows: ANGs as positive control, representing the clinical gold standard, were compared to chitosan/0.5% NVR-Gel conduits containing either naive nontransfected neonatal rat SCs (nt-neoSCs), empty vector transfected control SCs (tf-neoSCs-EV), GDNF overexpressing SCs (tf-neoSCs-GDNF), or FGF-2^{18kDa} overexpressing SCs (tf-neoSCs-FGF-2^{18kDa}). Nerve reconstruction by means of cell-free chitosan/0.5% NVR-Gel conduits was performed as an additional control. In order to assess the efficiency of peripheral nerve regeneration, functional and (histo-) morphometric parameters were evaluated.

Overall, the results obtained indicate a poor recovery through NVR-Gel-filled chitosan conduits in general, while 100% ANG-grafted animals functionally showed a high degree of motor recovery (detected by electrodiagnostical techniques) as well as almost complete recovery of mechanosensitivity (evaluated with von Frey algesimetry). However, delivery of FGF-2^{18kDa}-SCs significantly helped to overcome impediments for tissue regeneration and allowed functional recovery in 57% of the animals, emphasizing the role of this factor regarding promotion of peripheral nerve regeneration.

MATERIALS AND METHODS

Cell Culture

Neonatal Rat Schwann Cells. Primary culture of neonatal rat SCs (neoSCs) was performed as described previously (30). Briefly, sciatic nerves were harvested from Hannover Wistar rat pups (P1-3, in-house breeding) and enzymatically digested for 50 min. Cells were cultured for 24 h in DMEM, 1% P/S, 2 mM L-glutamine, 1 mM sodium pyruvate, and 10% fetal calf serum (FCS;

all PAA Laboratories, Coelbe, Germany) on poly-L-lysine (PLL)-coated culture flask (PLL; Sigma-Aldrich, Munich, Germany). After a 2-day period of incubation with 1 mM of arabinoside-c (Sigma-Aldrich) neoSC purity was increased by removing contaminating fibroblasts via immunopanning with magnetic Dynabeads® (Dynal Biotec ASA, Oslo, Norway) coupled to anti-Thy-1 antibodies (own production from hybridoma cell line); neoSCs were then seeded into a new PLL-coated culture flask. The purification procedure was repeated once or twice until >90% purity of neoSC cultures was reached; subsequently medium 2 μM Forskolin (PAA) was added to the medium for culture expansion.

NVR-Gel (NVR Labs Ltd., Ness-Ziona, Israel proprietary) was used as a layer for seeding of neoSCs in coculture with PC-12 cells (see below) or dissociated DRG cells (see below). Therefore, the NVR-Gel of 1% was mixed 1:1 with PC-12 differentiation medium (see below) or N2 medium (see below), respectively, to a final concentration of 0.5%.

Rat Pheochromocytoma Cell Line (PC-12 Cells). PC-12 cells [kindly provided by Dr. R. Westermann, Marburg, Germany, as described previously (27)] were expanded in proliferation medium (DMEM high glucose + 10% horse serum + 5% FCS + 4 μM L-glutamine + 1 μm sodium pyruvate + 100 U/ml penicillin/streptomycin (Pen/Strep; all Gibco, Darmstadt, Germany), and for neuronal differentiation experiments, the medium was changed to differentiation medium (DMEM + 1% horse serum + 1% FCS + 4 μM L-glutamine + 1 μm sodium pyruvate + 100 U/ml Pen/Strep).

Primary Dissociated Dorsal Root Ganglion (DRG) Cells. As described previously (76), DRGs were dissected from neonatal Hannover Wistar rat pups (P1-P3, in-house breeding) and collected in HBSS medium (PAA) and incubated in HBSS, 0.125% trypsin, 0.1% DNase (Roche GmbH, Mannheim, Germany) for enzymatic digestion over 20 min at 37°C. A following 25-min period of digestion with 0.0075% collagenase IV (0.1% stock; Worthington Biochemical Cooperation, CellSystems GmbH, Troisdorf Germany) was stopped by adding N2 medium [DMEM/F-12, 1×N2 supplement + 1% Pen/Strep + 2 mM L-glutamine, 1 mM sodium pyruvate + 0.25% bovine serum albumin (BSA; PAA) with 3% FCS (PAA)]. Finally, DRG cells were mechanically dissociated to a homogenous suspension using a fire-polished glass Pasteur pipette.

Nonviral Genetic Engineering of Cells

Both SCs and PC-12 cells were genetically modified using the AMAXA nucleofection technique (Amaxa device II; Lonza, Cologne, Germany). Nonviral plasmids were derived from the pCAGGS-empty vector as described previously (57) and as follows: plasmids encoding for enhanced green fluorescent protein (EGFP; pCAGGS-EGFP-Flag) and low molecular weight FGF-2 (pCAGGS-FGF-2-^{18kDa}-Flag; NCBI GenBank accession NM_019305.2, 533–994 bp) as described in Ratzka et al. (61), and the plasmid encoding for GDNF (pCAGGS-GDNF-Flag) was constructed by PCR-based cloning of the rat GDNF coding sequence (NCBI GenBank accession NM_019139.1, 50-682 bp) by Dr. Andreas Ratzka as described elsewhere (53). The in-frame cloned c-terminal 3× Flag tag of the pCAGGS-Flag vector backbone enabled convenient detection of all three proteins (EGFP-Flag, FGF-2-^{18kDa}-Flag, and GDNF-Flag) with the same antibody.

After transfection, cell survival was determined for a cell aliquot by trypan blue (Sigma-Aldrich) staining in the Neubauer chamber system (Carl Roth & Co GmbH, Karlsruhe, Germany). For transfection, 2.5×10^6 cells were suspended in 90 μl basic transfection solution (basic glial cell nucleofection kit for SCs or cell line nucleofection kit for PC-12 cells; both Lonza) and mixed with 5 μg of the respective plasmid DNA. Nucleofection occurred in AMAXA-specific cuvettes using the program T20 (SCs) or U29 (PC-12 cells). The reaction was stopped by adding 900 μl RPMI medium (Gibco) supplemented with 10% FCS, after which the cells were processed into the in vitro or in vivo experiments described below.

In the current study, we used for in vitro and in vivo studies 1) nontransfected neoSCs (nt-neoSCs), and the following genetically engineered SC types: 2) empty vector transfected SCs (tf-neoSCs-EV), 3) EGFP-expressing neoSCs (EGFP-neoSCs), 4) GDNF overexpressing neoSCs (tf-neoSCs-GDNF), and 5) FGF-2^{18kDa} overexpressing neoSCs (tf-neoSCs-FGF2^{18kDa}). For in vitro studies, we further used (B) EGFP-expressing PC-12 cells (EGFP-PC-12).

Protein Detection by SDS Gel Electrophoresis and Western Blot Analyses

Overexpression of FGF-2^{18kDa} and GDNF by tf-neoSCs (passages 5–9) was confirmed in Western blot analyses. Therefore, cell culture supernatants were collected and cell lysates prepared in 1% sodium dodecyl sulfate buffer (SDS; Roth GmbH) prior to denaturation at 95°C and sonification for 15 min. For each sample, a calculated protein concentration of 50 μg was prepared in 2× Laemmli buffer 1970 (5×, 0.25 M Tris HCl pH 8.0, 25% glycerol, 7.5% SDS, 0.25 mg/ml bromphenol blue, 12.5% v/v mercaptoethanol; all Sigma-Aldrich). Following SDS polyacrylamide gel electrophoresis (15% gels), the separated proteins were transferred to a nitrocellulose membrane (RPN68D; Amersham Bioscience, Freiburg, Germany) by electrophoresis (62). Following immune detection of FGF-2^{18kDa}, GDNF, or Flag-Taq in the ECL system (Intas Science Imaging, Göttingen, Germany) using monoclonal anti-FGF-2 (1:1,000, 05-118; Merck Millipore, Merck

KGaA, Darmstadt, Germany) antibody, polyclonal anti-GDNF (1:200, sc328; Santa Cruz Biotechnology Inc., Heidelberg, Germany) antibody or anti-Flag (1:3,000, F18-04; Sigma-Aldrich) antibodies, incubation with the secondary horseradish peroxidase (HRP)-coupled antibodies (1:4,000, NA931V or NA934V; Amersham Bioscience Europe, Freiburg, Germany) was performed. Protein signals were visualized with a substrate solution (WBKLS0500, Immobilon; Merck Millipore).

Neuronal Differentiation of PC-12 Cells Induced by Genetically Different NeoSCs

Induction of neurite formation by EGFP-PC-12 cells in coculture with nt-neoSCs or tf-neoSCs-FGF-2^{18kDa} was compared to that induced by recombinant human FGF-2 (17.2 kDa) (100-18B; PeproTech GmbH, Hamburg, Germany). Therefore, 30×10^4 EGFP-PC-12 cells were mixed with 40×10^4 neoSCs prepared in their cell-specific culture medium and transferred in a volume of 1 ml in 0.5% NVR-Gel (1:1 in PC-12 differentiation medium) for seeding into a 24-well plate (Nunc; Thermo Fisher Scientific, Schwerte, Germany). For control conditions, 50 ng/ml FGF-2^{18kDa} was added to PC-12 differentiation medium, which was mixed with NVR-Gel to a final concentration of 0.5% before EGFP-PC-12 cells were added. After 5 days in vitro (DIV 5), cells were fixed with 6% paraformaldehyde (PFA; Sigma-Aldrich) and microscopically analyzed using Cell P (Olympus IX70, Hamburg, Germany). The analysis was performed in three independent biological replicates.

Neurite Outgrowth From Dissociated DRG Cells Induced by Genetically Different NeoSCs

A number of 40×10^4 nt-neoSCs, tf-neoSCs-GDNF, or tf-neoSCs-FGF-2^{18kDa} were suspended in 1 ml 0.5% NVR-Gel (1:1 with N2 medium) and plated into a 24-well plate. After 24 h, 2.5×10^3 freshly dissociated DRG cells were placed as a drop in the middle of the neoSC-containing NVR-Gel layer. After an additional 24 h, the cultures were fixed with 6% PFA and processed for immunocytochemistry. Unspecific antibody binding sites were blocked with phosphate-buffered salt solution (PBS; Biochrom, Berlin, Germany)/0.3 Triton X-100 (Roche GmbH)/3% normal goat serum (NGS; Gibco)/2% bovine serum albumin (BSA; PAA) solution for 1 h at room temperature (RT). This was followed by overnight incubation with neuron-specific anti-β-III-tubulin antibody (1:400, ab78078; Abcam, Cambridge, UK) and SC-specific anti-S100 antibody (1:1,000, Z0311; Dako, Glostrup, Denmark) in PBS/0.3%Triton X-100/1% NGS/1%BSA at 4°C. The staining was finalized by an incubation with Alexa-555-labeled goat anti-mouse IgG secondary antibody and Alexa 488-labeled goat anti-rabbit secondary (both 1:500; Invitrogen, Darmstadt, Germany) for ~1.5 h at RT. All cell nuclei were counterstained with the nuclear dye 4′,6′-diamino-2-phenylindole (DAPI, 1:1,000 in PBS; Sigma-Aldrich). Neurite morphology was analyzed in fluorescence microscopy (Olympus IX70), and for every experimental setting, eight single photomicrographs were digitalized in 4× magnification and analyzed in a merged picture using ImageJ software (NIH, Bethesda, MD, USA). For each sample, the perimeter of the DRG drop was manually drawn (Polygon selection tool) and automatically enlarged (Edit-Selection-Enlarge tool) to create concentric curves at a fixed distance (from 500 to 1,100 µm) between each other. The number of intersections of neuritic processes with the different curves was then counted and represented as mean values. Additionally, the maximum neurite lengths originating from the DRG drop cultures were analyzed for the 10 longest neurites. The analysis was performed in three independent biological replicates.

Manufacturing of Chitosan Conduits

Extraction of medical-grade chitosan from *Pandalus borealis* shrimp shells was performed by Altakitin S.A. (Lisbon, Portugal). Chitosan conduits with a degree of acetylation of 5% were produced by Medovent GmbH (Mainz, Germany) following a protocol of repeated washing and hydrolysis steps as described previously (34). All manufacturing processes were in accordance with ISO 13485 requirements and specifications.

Preparation of Genetically Engineered NeoSCs for Transplantation Within Composite Chitosan Nerve Conduits

To analyze the metabolic viability, the protein expression levels, and the cellular distribution within composite nerve conduits, immediately after eventual transfection, 1×10^6 genetically different neoSCs (nt-neoSCs, tf-neoSCs-FGF-2^{18kDa}, tf-neoSCs-GDNF) were suspended in 0.5% NVR-Gel prepared with serum-free N2 medium. The cell-seeded composite conduits were placed into cell culture plates and additionally covered with 1 ml of 0.5% NVR-Gel in order to avoid drying of the conduits and incubated until follow-up evaluation in humidified atmosphere with 5% (v/v) CO_2.

For transplantation into our animal model, 2.5×10^6 neoSCs (passages 8–10) were genetically modified as described above 3 days prior to surgery. The cells were then cultured for 24 h on PLL-coated six-well plates (Nunc; Thermo Fisher Scientific) in SC-specific culture medium to recover from transfection. On the same day, the medium was changed to serum free-N2 medium. After an additional 24 h, a total of 1×10^6 genetically different neoSCs (passages 8–9) were mixed with 0.5% NVR-Gel (110 µl first set of surgeries and 130 µl second set of surgeries) and transferred into chitosan tubes. The conduits

were placed into cell culture plates and additionally covered with 1 ml 0.5% NVR-Gel and incubated overnight at 37°C in humidified atmosphere with 5% (v/v) CO_2. On the following day, conduits containing genetically different neoSCs: nt-neoSCs, tf-neoSCs-EV, tf-neoSCs-GDNF, tf-neoSCs-FGF-2^{18kDa} were transplanted into rat sciatic nerve defects as described below.

In order to determine neoSCs purity and transfection rates for the transplanted neoSCs, residual cells were cultured for immunocytochemical analysis (50×10^4 cells/24-wells, $n = 2$ wells/neoSCs type). For monitoring SC purity, sample sister cultures were stained for anti-S100. The transfection rates were determined with anti-Flag-staining (1:200, F1804; Sigma-Aldrich)/anti-Alexa 555 (1:500), cell nuclei were counterstained with the nuclear dye DAPI (1:1,000 in PBS; Sigma- Aldrich).

For metabolic viability measurements a WST-1 assay (Roche GmbH) was performed as previously described (76), neoSCs were flushed out of composite chitosan conduits ($n = 3$/condition) after 24 h and seeded into PLL-coated 24 wells in N2 medium supplemented with 3% FCS. Cell adhesion was allowed to take place for 1.5 h before the medium was removed and substituted by the WST-1 solution mixed 1:10 with N2 medium. A volume of 350 µl was added to each well. After 3.5 h of incubation, the reduced solution was transferred in triplicates into a 96-well plate (Nunc; Thermo Fisher Scientific) and measured at 450 nm.

To evaluate the protein expression of neoSCs 24 h after transferring them into composite chitosan conduits ($n = 3$ conduits/condition), the cells were also flushed out with N2 medium and centrifuged, the pellets were washed with PBS and centrifuged another time before the pellets were stored at −80°C prior to Western blot analysis as described above.

To analyze the cellular distribution within the composite chitosan tubes, EGFP-neoSCs suspended in 0.5% NVR-Gel were transferred into the conduits and consecutively monitored with fluorescence microscopy (Olympus IX70) for up to 9 days (DIV 1, 5, and 9) in vitro.

Animals and Surgical Procedure

All animal experiments followed the German Animal Protection Act and were approved by the local animal protection committee (Animal care committee of Lower Saxony). Adult female Wistar rats (225–250 g) were obtained from Janvier [Genest Saint Isle (Le), France] and housed in groups of four under standard conditions (RT 22.2°C; humidity 55.5%; light–dark cycle 14 h/10 h). Food and water were available ad libitum for the complete duration of the experiments.

During surgery and electrodiagnostic recordings, the rats were generally anesthetized by an intraperitoneal injection of chloral hydrate (370 mg/kg; Sigma-Aldrich), and sufficient analgesia was ensured by intramuscular injection of buprenorphine (0.045 mg/kg, Buprenovet®; Bayer Pharmaceuticals, Lerverkusen, Germany). On the 2 days following the initial surgery, the animals also received butorphanol tartrate (0.5 mg/kg, Torbugesic®; Pfizer GmbH, Berlin, Germany) via subcutaneous injection as pain relief. Additionally, amitriptyline hydrochloride (9 mg/kg/day, Amitriptylin-neuraxpharm®; Neuraxpharm Arzneimittel GmbH, Langenfeld, Germany) was administered through the drinking water, starting 2 weeks prior to the surgery until the end of the observation period to minimize eventual automutilation events (55).

Animals were prepared for surgery as described previously (34). In short, the left sciatic nerve was exposed under sterile conditions and the wound was kept open using small self-made retractors similar to the technique described by Bozkurt et al. (12). The gluteus muscle served as a landmark to allow transection of the sciatic nerve at a constant point. Five millimeters of the distal nerve end was removed, and composite chitosan conduits (length 19 mm) were implanted to bridge a critical nerve defect of 15 mm length. In control animals, a reversed ANG was implanted. Therefore, the distal nerve end was transected 15 mm distal to the first transection point again, and the free nerve segment was then flipped to reverse its proximodistal orientation and turned 90° around its longitudinal axis before three sutures (9-0, EH7981G, Ethilon; Ethicon, Livingston, Scotland) were located 120° apart from each other. Besides the ANG control group, four experimental groups were analyzed in which the composite chitosan nerve conduits contained 1) nt-neoSCs, 2) tf-neoSCs-EV, 3) tf-neo-SCs-GDNF, and 4) tf-neoSCs-FGF-2^{18kDa}. Surgeries were performed on consecutive days in two series ($n = 4$/condition/series). In a parallel experiment (performed by Shimon Rochkind at Tel-Aviv Sourasky Medical Center, Israel), one group of additional animals ($n = 10$) received chitosan nerve conduits filled with 0.5% pure NVR-Gel. On these nerve samples only morphological analysis was performed.

Assessment of Functional Recovery

Progress of functional recovery was monitored by calculation of the Static Sciatic Index [SSI, as described previously (40)], assessment of the mechanical pain threshold via von Frey test, serial noninvasive electrophysiological measurements, as well as by calculation of the lower limb muscle weight ratio upon sacrifice. The investigators were blinded to the nerve reconstruction conditions.

Assessment of the Mechanical Pain Threshold (Von Frey Test). Plastic compartments were positioned on a metallic mesh stand and animals were placed inside the boxes and allowed to acclimate to the surrounding for 15 min. Following habituation, a blunted needle connected to a force sensor in a handheld probe (electronic von Frey

algesimeter; IITC Inc. Life Science, Woodland Hills, CA, USA) was used to stimulate the medial and lateral side of the plantar surface of the intact and injured paw. Pressure was increased gradually and slowly until withdrawal of the examined paw. The applied force needed to induce a paw-lifting reaction was displayed as the weight force (g). A cutoff value was set to 40 g. This value was also noted when no active withdrawal reaction was detectable. The paw withdrawal pressure was recorded five times for each side, with an interval between the stimuli of at least 3 min, and the three steadiest values were used for calculation of a mean that was then used for statistical analysis. The test was performed three times before surgery for habituation and repeated at 1, 4, 9, 12, and 16 weeks after it.

Serial Noninvasive Electrodiagnostic Recordings. Muscle reinnervation was analyzed through noninvasive electrodiagnostic measurements 9, 13, and 17 weeks after nerve reconstruction as described previously (34). In short, a portable electrodiagnostic device (Keypoint Portable; Medtronic Functional Diagnostics A7S, Skovlunde, Denmark) was used to stimulate the sciatic nerve with single electrical pulses (100 μs duration and supramaximal intensity) by transcutaneous placement of monopolar needles (30 G, diameter 0.3 mm, length 10 mm; Natus Europe GmbH, Planegg, Germany). For the recordings, the animals were placed and fixed in a standardized prone position with the hindlimbs extended. Stimulation electrodes were always put at the same landmarks: proximal electrodes at the sciatic notch and distal electrodes into the popliteal fossa. The distance between the proximal and distal stimulation points was used to calculate the nerve conduction velocity (NCV). Recording electrodes were inserted into the tibialis anterior (TA) or plantar (PL) muscles to detect evoked compound muscle action potentials (CMAPs). The data gained from successful recordings were used to calculate the NCV ratio, area under the curve, and amplitude ratio, with the latter two providing information with regard to functional axon loss or recruited axons, respectively. NCV and amplitude ratios were calculated by using values obtained from the healthy side as reference (ipsilateral lesioned side/contralateral healthy side).

Muscle Weight Ratio. The TA muscles as well as gastrocnemius muscles of all animals were harvested after finalizing the functional tests and their fresh (wet) weight was noted to calculate the muscle weight ratio (ipsilateral lesioned side/contralateral healthy side).

Histological Evaluation

The animals were sacrificed (in deep anesthesia in a CO_2 atmosphere with final cervical dislocation), and connective tissue or peripheral nerve tissue was subjected to fixation by immersion in specific solutions as described in the following, since transcardial perfusion was not found obligatory for the chosen evaluations.

Analysis of Connective Tissue Surrounding the Nerve Conduits. Connective tissue that had developed around the different composite nerve conduits was explanted ($n = 4$–6 each group) and prepared for histological analysis as described previously (34). Seven-micrometer-thick sections were cut from the distal end of the samples, and four sections within a distance of 300 μm were subjected to hematoxylin and eosin (H&E) staining (Roth GmbH) and analyzed with regard to number of multinucleated giant cells (MGCs), tissue thickness, and area. Additional two sections obtained from the distal end, covering a distance of approximately 300 μm, were stained for activated macrophages. Therefore, paraffin cross sections were incubated in PBS with 3% milk powder (Heirler Cenovis GmbH, Karlsruhe, Germany) and 0.5% Triton X-100 for blocking before incubation with primary mouse anti-ED1 antibody (1:1,000 in blocking solution, MCA341R; AbD Serotec, Puchheim, Germany) at 4°C overnight. After washing in PBS and incubation with Alexa 555-conjugated secondary goat-anti-mouse antibody (1:1,000; Invitrogen) for 1 h at RT, counterstaining with DAPI (1:2,000) was performed for 2 min at RT. Finally, the stained samples were mounted with Mowiol (475904; Calbiochem, San Diego, CA, USA). Four photomicrographs per section were acquired (IX70 microscope; Olympus), and cell counting was performed as described previously using ImageJ software (NIH, Bethesda, MD, USA) (34).

Assessment of the Regenerated Nerve Tissue. Regenerated nerve tissue was carefully removed from the surrounding chitosan and fixed in 4% PFA (overnight at 4°C) for subsequent paraffin embedding and (immuno-) histological analysis. Chitosan conduits only containing thin regenerated tissue were left intact, eventually with connective tissue around and entirely processed for paraffin embedding. Furthermore, in cases of failed regeneration, single proximal nerve stumps were processed for histological analysis.

Seven-micrometer cross sections obtained from samples showing clear tissue regeneration as well as representative proximal nerve stumps gained from cases of failed regeneration were cut starting from the distal end, covering a distance of approximately 600 μm. After discarding a 1.5-mm piece of the sample, a second series of 600 μm was cut and gathered for histological analysis. Exemplary samples of thin as well as failed tissue regeneration were additionally cut in the middle of the tube, and sections were gathered covering a distance of about 300 μm.

Two sections of each series were H&E stained and evaluated with regard to the number of MGCs, while

adjacent sections were subjected to ED1 and NF200 staining to enable counting of activated macrophages and visualizing of regenerated axons. For the latter, sections were subjected to ED1 staining as described above followed by a second blocking step and subsequent overnight incubation with primary rabbit anti-NF200 antibody (1:500; N4142; Sigma-Aldrich). After washing, incubation with Alexa 488-conjugated secondary goat-anti rabbit antibody (1:1,000; Invitrogen) for 1 h at RT and counterstaining with DAPI (1:2,000) was performed

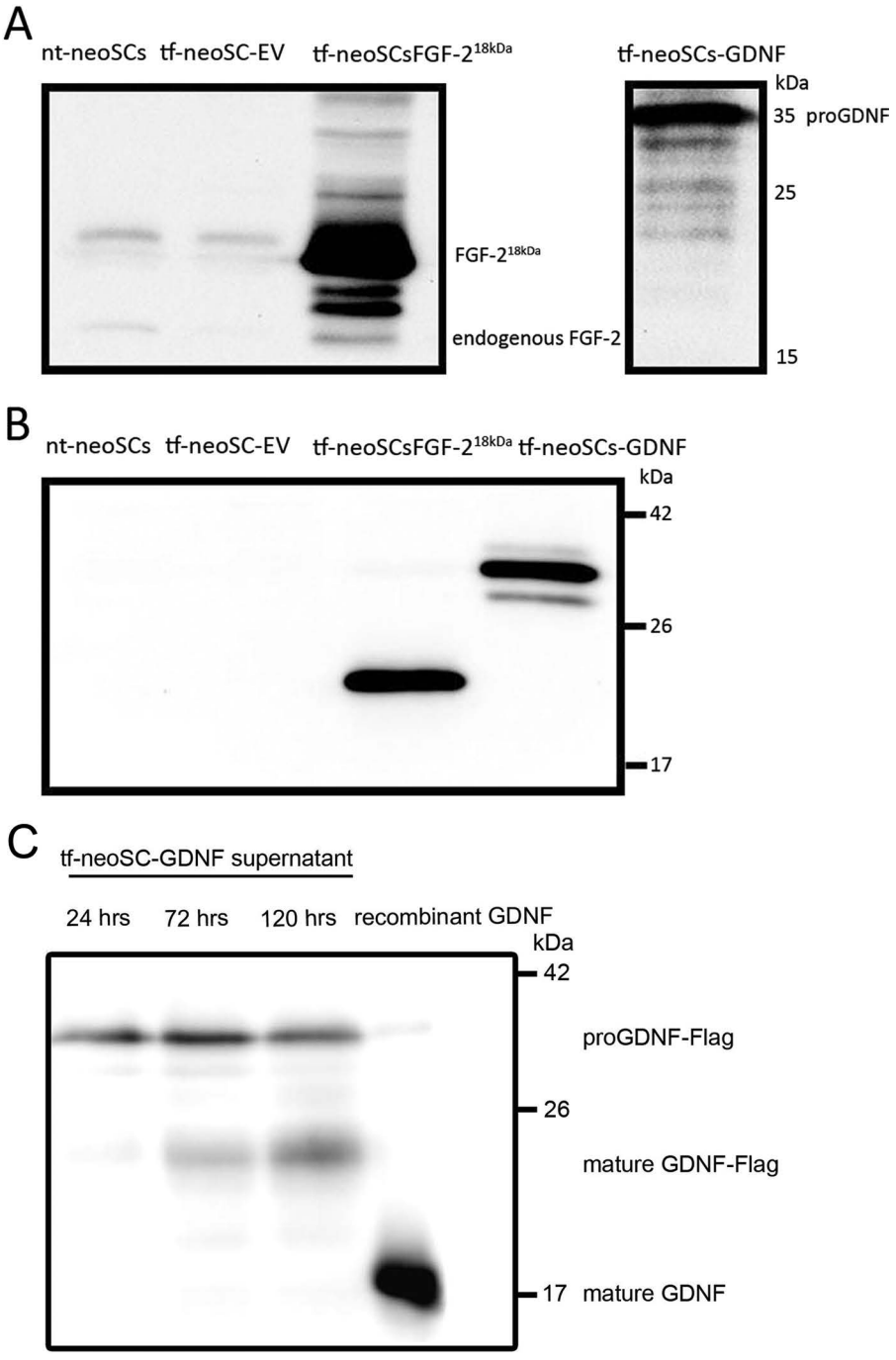

Figure 1. Results of Western blot analysis of cell lysates from naive or genetically engineered Schwann cells. Detection of FGF-2^{18kDa} and pro-GDNF overexpression by Western blot analyzes of cell lysates from nt-neoSCs, tf-neoSCs-EV, tf-neoSCs-FGF-2^{18kDa}, or tf-neoSCs-GDNF (A) cultured for 24 h in regular culture conditions or (B) flushed out of composite chitosan tubes 24 h after seeding and 48 h after transfection. (C) Mature GDNF was detected in cell culture supernatants from genetically modified neoSC after 72 h and 120 h. Each $n=3$.

prior to section mounting. Up to five images (magnification: 20×) were acquired per section (depending on the sample diameter), and counting of activated macrophages was performed with the help of ImageJ software.

Nerve Morphometry. Segments of 5-mm lengths were cut off the distal nerve segment at 2 mm distal to the distal suture site and processed for myelin staining and araldite resin embedding and stereological analysis as described previously (22,34). Therefore, the harvested tissue was subjected to a fixation according to Karnovsky (2% PFA and 2.5% glutaraldehyde in 0.2 M sodium cacodylate buffer) prior to postfixation in 1% OsO_4. Following dehydration in an ethyl alcohol row, the samples were delivered to the partner laboratory at the University in Turin for embedding in a mixture of Araldite resin. Semithin cross sections of samples of the functionally recovered nerves were subjected to morphometric analysis in order to determine the mean total number of regenerated myelinated axons in the nerve segment distal to the reconstructed nerve gap as well as the mean nerve fiber density, the mean axonal diameter, fiber diameter, myelin thickness, and g-ratio. Additionally, the same analysis was performed on 10 distal nerve segments from healthy contralateral nerves of the animals included in this study.

Statistical Analysis

The data obtained were subjected to Kruskal–Wallis test or two-way ANOVA (analysis of variance) followed by Dunn's or Tukey's multiple comparisons test (GraphPad Prism 6) as indicated in the Results section. Results are presented as median ± range or mean ± standard error of the mean (SEM) and p values were set at $p<0.05$, $p<0.01$, and $p<0.001$ as level of significance.

RESULTS

Prior to modifying hollow chitosan conduits with the luminal filler, 0.5% NVR-Gel containing neoSCs as a drug delivery system, we evaluated the expression levels of the proteins of neoSCs 24 h after transfection and regular culture as well as 24 h after seeding them into composite chitosan conduits (48 h after transfection) in Western blot analysis. Successful overexpression of FGF-2^{18kDa} and GDNF was revealed by strong bands in Western blots from cell lysates of both regular cell cultures (Fig. 1A) and composite chitosan conduits (Fig. 1B), while endogenous FGF-2^{18kDa} expression was only detected at very low levels in cell lysates from cultured nt-neoSCs and tf-neoSCs-EV. Regarding the overexpression of GDNF, an additional analysis was performed because cell lysate analysis 24 h and 48 h after transfection revealed strong bands mainly for pro-GDNF. To demonstrate that also the expression of mature GDNF is increased, we cultured tf-neoSCs-GDNF for up to 120 h and detected GDNF levels within the cell culture supernatant (Fig. 1C). Five days after transfection, not only pro-GDNF but also mature GDNF have been released into the cell culture supernatant in detectable amounts. The secretion of pro-GDNF earlier to the fully processed protein is very likely dependent on the plasmid transfection performed. In contrast to previous descriptions about GDNF synthesis as a precursor and secretion as a mature protein, recent studies documented its secretion also as unprocessed pro-GDNF in cell culture due to plasmid transfection (47,60,67).

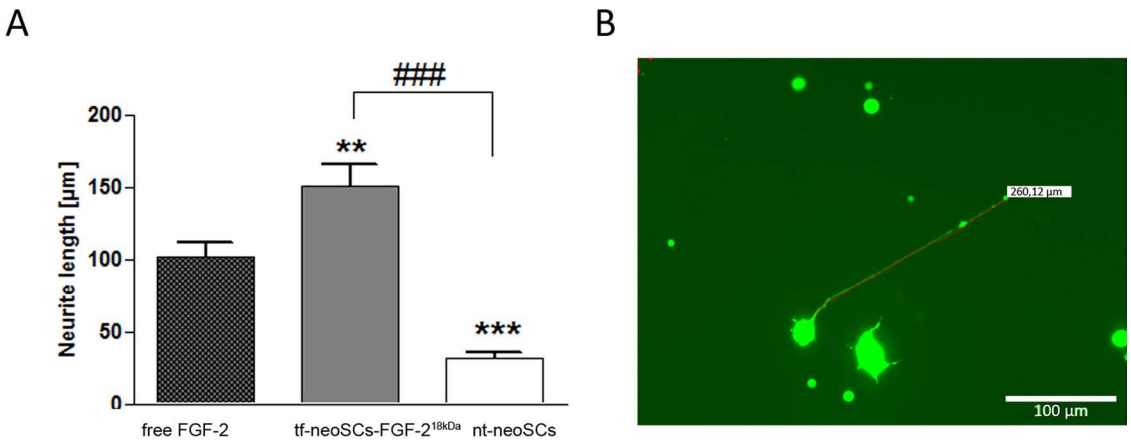

Figure 2. Results of the PC-12 cell neurite outgrowth assay. (A) Bar graph presenting lengths of induced neurite formation by EGFP-PC-12 cells in NVR-Gel supplemented with 50 ng/ml of free recombinant FGF-2 or cocultured with nt-neoSCs or tf-neoSCs-FGF-2^{18kDa}. Mean ± SEM, $n=3$, **$p<0.01$, ***,### $p<0.001$, one-way ANOVA with Tukey's multiple comparison test; ** and ***differences to free recombinant FGF-2; ###differences between nt-neoSCs and tf-neoSCs-FGF-2^{18kDa}. (B) Sample photomicrograph demonstrating long neurite formation of an EGFP-PC-12 cell in the presence of tf-neoSCs-FGF-2^{18kDa}.

Genetically Engineered tf-neoSCs Demonstrate Neurite Inductive Bioactivity in 3D-NVR-Gel-Based Culture Systems

Two cell culture models were used to evaluate the bioactivity of genetically engineered neoSCs embedded in 0.5% NVR-Gel. In the PC12-cell neuronal differentiation model, we assessed a traditional sympathetic neuronal cell line in a classic neurite outgrowth assay (73), while we evaluated sensory neuron outgrowth with our dissociated DRG cell drop cultures.

In the PC-12-neurite outgrowth assay, we exclusively evaluated the bioactivity of nt-neoSCs and tf-neoSCs-FGF-2^{18kDa} and compared it to the bioactivity of free recombinant FGF-2 because PC-12 cells are not sensitive to GDNF. As demonstrated in Figure 2A, free recombinant FGF-2 induced significantly increased neurite outgrowth by PC-12 cells when compared to nt-SCs. The neuronal differentiation was further significantly increased when PC-12 cells were cultured together with tf-neoSCs-FGF-2^{18kDa} (Fig. 2A, B).

In the DRG drop culture model, however, no significant difference in the neurite inductive effects between nt-neoSCs or tf-neoSCs were detectable, irrespective of if DRG drops were cultured in the presence of tf-neoSCs-GDNF or tf-neoSCs-FGF-2^{18kDa}. Both the numeric neurite outgrowth at certain distances from the dissociated DRG cell drop cultures (Fig. 3A) and the maximum neurite length extending from them (Fig. 3B) were comparable in all culture conditions. A sample culture in the presence of tf-neoSCs-FGF-2^{18kDa} is shown in Figure 3C.

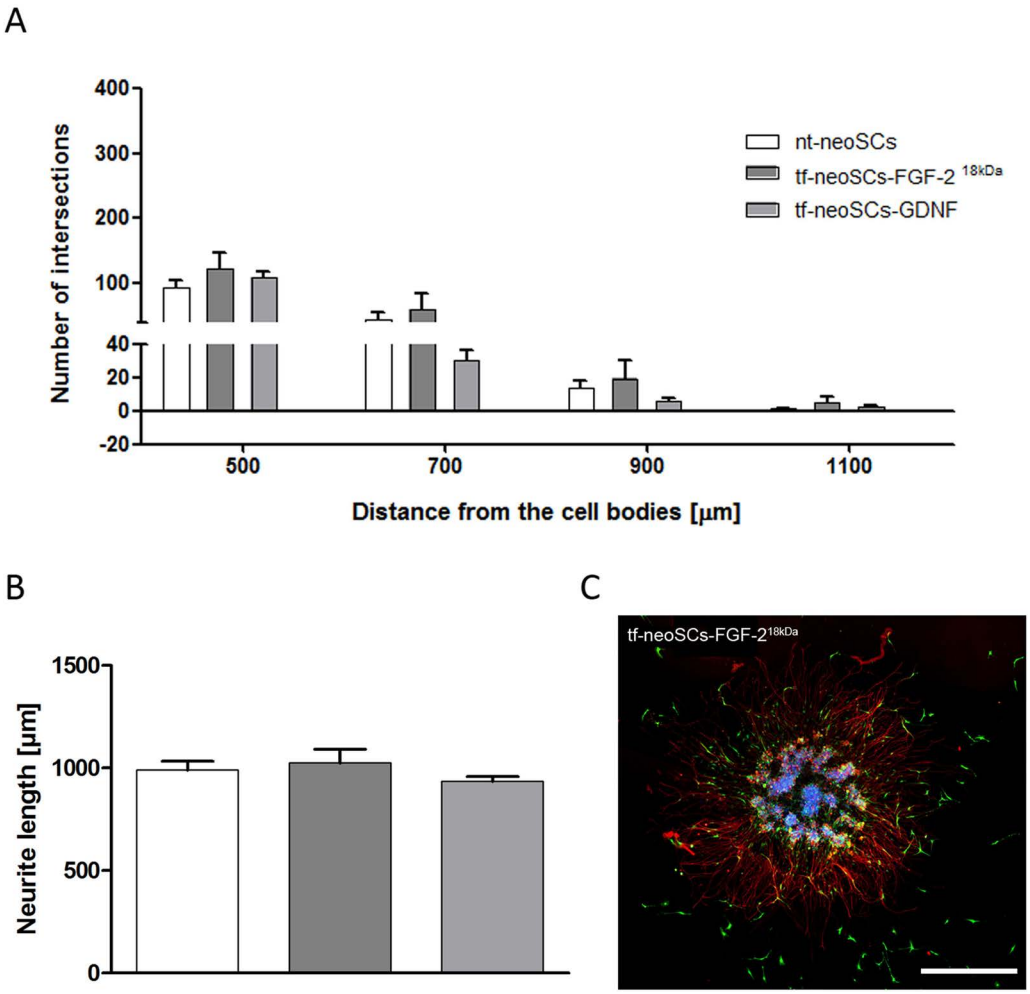

Figure 3. Results of the neonatal dorsal root ganglion neurite outgrowth assay. (A) Neurite outgrowth of dissociated sensory DRG cell drop cultures was evaluated according to the number of intersections (*y*-axis) and the distance of the neurites grown from the drop perimeter (*x*-axis). (B) Mean length (±SEM, $n=3$) of the 10 longest neurites extending from the DRG drop cultures. (C) Sample photomicrograph of a fluorescence-labeled DRG drop (stained for β-III tubulin, red) cocultured with tf-neoSCs-FGF-2^{18kDa} (S-100, green); all cell nuclei were counterstained with DAPI (blue).

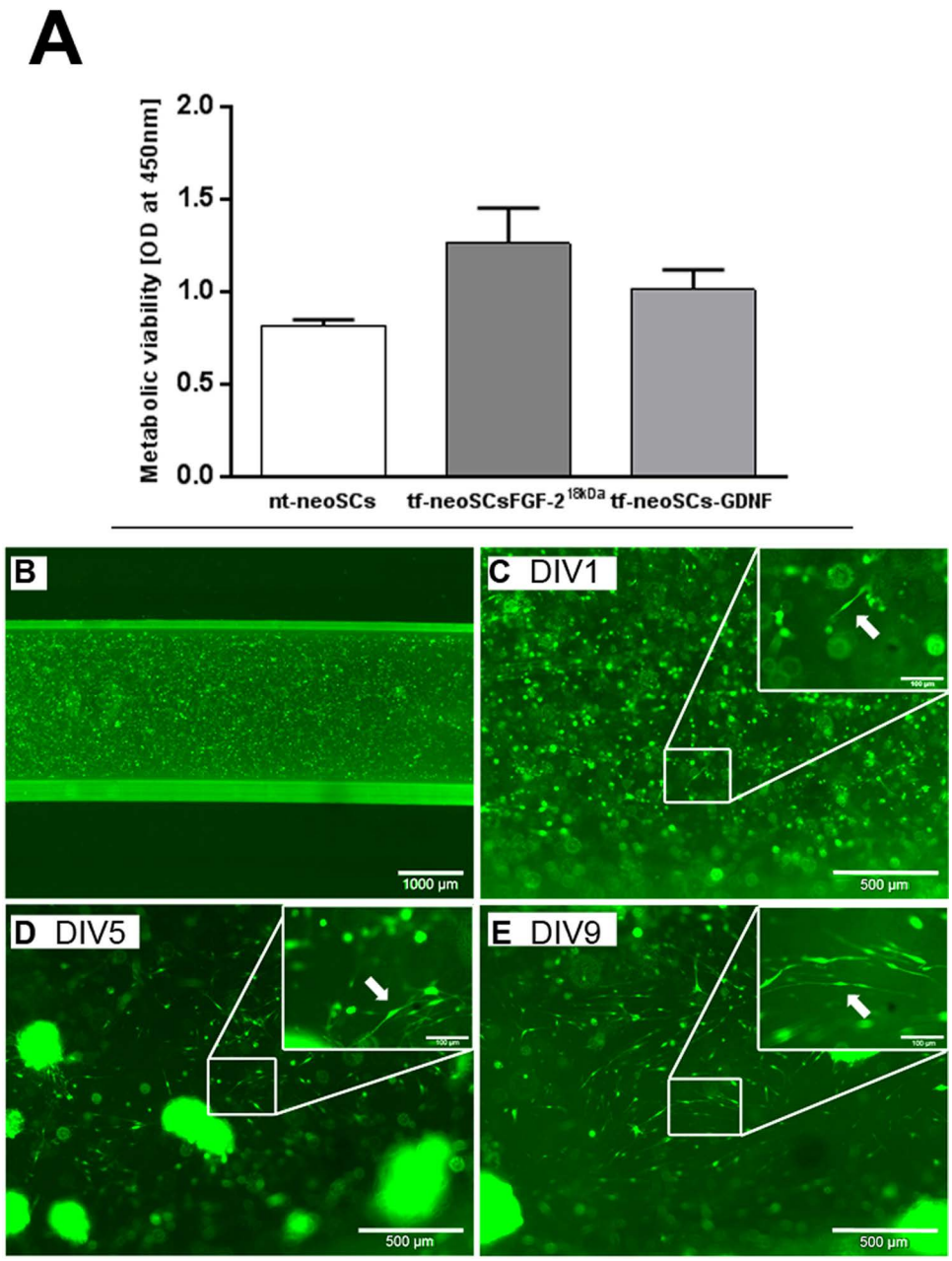

Figure 4. Metabolic activity and morphology of naive and genetically engineered Schwann cells in NVR-Gel-filled chitosan nerve guides in vitro. (A) Bar graph depicting the metabolic viability of nt-neoSCs, tf-neoSCs-FGF-2^{18kDa}, and tf-neoSCs-GDNF, which have been flushed out from composite chitosan nerve conduits 24 h after seeding (mean ± SEM, $n = 3$ conduits per condition). (B–E) Cell morphology and distribution of neo-SCs within the composite nerve conduits was monitored after seeding of EGFP-neoSCs for up to 9 days in vitro. Arrows point to EGFP-neoSCs migrating out of initially formed cell clusters when they also demonstrate their typical bipolar morphology.

Genetically Engineered tf-neoSCs Demonstrate Sufficient Metabolic Viability, Develop Their Typical Morphology, and Migrate Within NVR-Gel-Enriched Composite Chitosan Conduits In Vitro

Analysis of the WST-1 assay performed 24 h after seeding nt-neoSCs or tf-neoSCs into NVR-Gel-filled chitosan conduits revealed overall metabolic active and viable neoSCs (Fig. 4A). The metabolic activity of tf-neoSCs was slightly increased over that of nt-neoSCs with the strongest reaction seen for tf-neoSCs-FGF-2^{18kDa} (Fig. 4A). Analysis of the cell morphology of EGFP-neoSCs monitored over up to 9 days in vitro demonstrated aggregated round-shaped cells 24 h after seeding in an overview (DIV 1, Fig. 4B). In Figure 4C,

this is shown in higher magnification as well. At DIV 5 EGFP-neoSCs had migrated out of the initially formed cell clusters to populate the NVR-Gel-filled lumen of the chitosan tube showing their typical bipolar morphology (Fig. 4D). Upon final examination at DIV 9, even increased cell numbers with SC typical morphology were seen (Fig. 4E).

After we could demonstrate overexpression of bioactive target proteins by tf-neoSCs within composite chitosan nerve conduits together with sufficient cellular viability and equal distribution of the cells within the nerve conduits, we initiated the in vivo investigations.

Over a time period of 17 weeks, functional evaluation of the regeneration progress was performed. As experienced in other studies (34,46), the evaluation of the SSI after long nerve defect repair did not reveal any differences among the groups.

Early Sensory Reinnervation Events Were Detectable After Reconstruction With an Autologous Nerve Graft, While This Was Rare After Reconstruction With Composite Nerve Conduits.

The first signs of sensory recovery, indicated by the withdrawal response upon stimulation of the lateral plantar paw side of the lesioned hindlimb were detectable 9 weeks after nerve reconstruction in all ANG group animals. As depicted in Figure 5, the pressure, however, required to elicit this response was significantly decreased (12.64±1.26 g) compared to the values obtained from stimulation of the same area at the contralateral healthy paw (20.16±0.30 g), indicating hyperalgesia. At the same time, only single animals of the nt-neoSCs ($n=1$, 18.93 g), tf-neoSCs-GDNF ($n=1$, 20.93 g), and tf-neoSCs-FGF-2^{18kDa} ($n=1$, 15.60 g) groups demonstrated similar signs of reinnervation. Until the end of the observation period, no sensory recovery was seen in

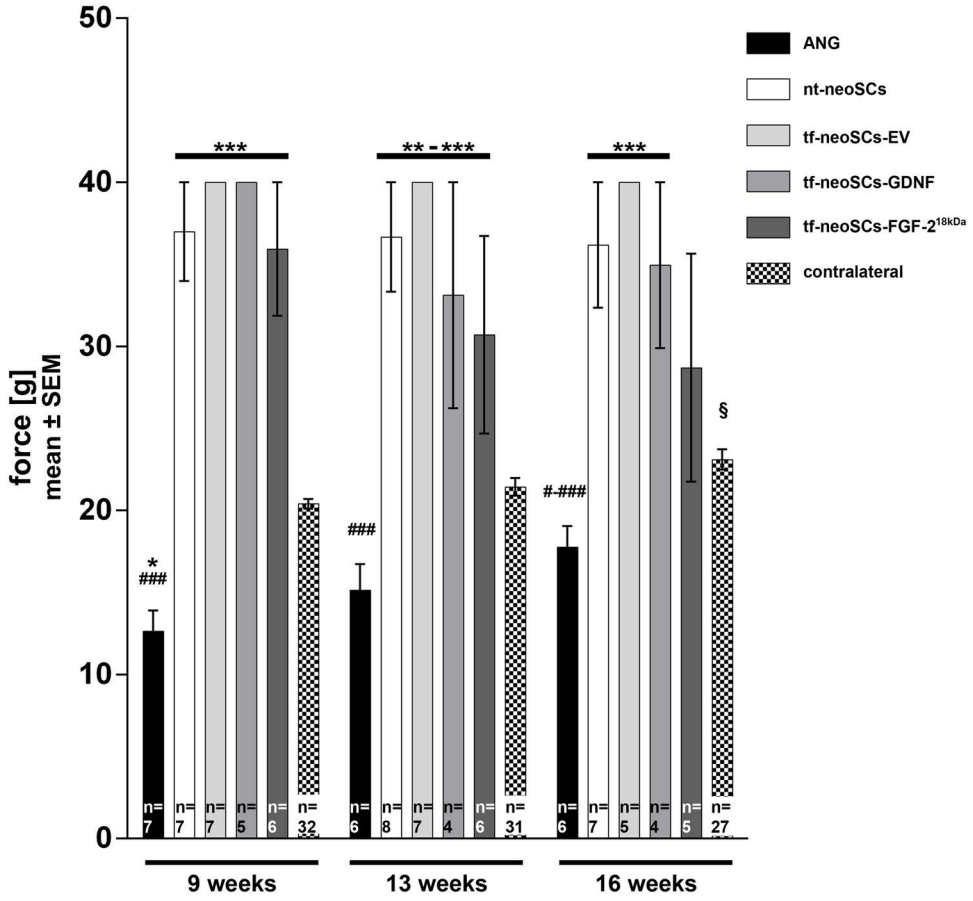

Figure 5. Results of the functional evaluation of mechanical pain thresholds with von Frey algesimetry testing. Bar graph illustrating the development of the mechanical pain threshold at the lateral plantar paw of the lesioned versus the contralateral healthy hindlimb over the recovery time within the different treatment groups (mean±SEM). Stimulation of the lateral territory revealed almost sole reinnervation in the ANG group, while only single animals responded in the other groups. For statistical analysis, all animals were included, and in case of no signal detection, cutoff force values (40 g) were set. Results were tested for significance ($p<0.05$) using two-way ANOVA, Tukey's multiple comparisons. *$p<0.05$, **$p<0.01$, ***$p<0.001$ versus values obtained from the contralateral side; #$p<0.05$, ##$p<0.01$, ###$p<0.001$ versus fellow experimental groups at the same time point, §$p<0.05$ versus tf-neoSCs-EV group at the same time point.

the tf-neoSCs-EV group, while in the ANG group the pain threshold increased with ongoing reinnervation until it no longer differed significantly from healthy control values of the contralateral side (week 12: 15.15±1.59 g; week 16: 17.76±1.28 g), representing recovery from initial hyperalgesia and reestablishment of normal mechanical sensation. Also the single animals of the other groups demonstrated an increase of the mechanical pain threshold with time after surgery, and exclusively in the tf-neoSCs-FGF-2^{18kDa} group, a second animal was detected with recovering mechanic pain sensation at the lateral plantar side of the paw of the lesioned hindlimb.

The pain threshold measured in response to stimulation of the medial plantar paw side of the lesioned hindlimb, a territory that is partly innervated by the saphenous nerve, was significantly decreased in all animals following nerve transection and repair compared to values obtained from the same area of the contralateral healthy paw. These signs of hyperalgesia did not recover during the observation period of 16 weeks.

Motor Recovery Was Sufficient After Autologous Nerve Grafting and Achieved a Notable Value Only After Transplantation of tf-neoSC-FGF-2^{18kDa} Within Composite Nerve Conduits.

Recovery of muscle innervation was evaluated by means of noninvasive nerve conduction tests at 9, 13, and 17 weeks after sciatic nerve transection and reconstruction. The results of these measurements are listed in Table 1 for the tibialis anterior (TA) muscles and in Table 2 for the plantar (PL) muscles. Nine weeks after surgery, reinnervation of the TA muscles as well as the PL muscles was already detectable in almost all animals of the ANG group, while it was only spotted in a single animal of the nt-neoSCs and tf-neoSCs-EV groups, respectively. Thirteen weeks after surgery, compound muscle action potentials (CMAPs) were evocable in all animals of the ANG group both from the TA and PL muscles. At the same time, the positive recording from one tf-neoSCs-EV animal was not confirmed, but a first animal of the tf-neoSCs-FGF-2^{18kDa} group showed signs of reinnervation. Finally, 17 weeks after surgery, CMAPs were

Table 1. Nerve Conduction Velocity, Axon Loss, and Recruited Axons as Calculated From the Tibialis Anterior (TA) Muscle Recordings

	Animals per Group	Amplitude Ratio	NCV Ratio	AxL (%)
9 weeks				
ANG	7/8	0.2±0.03 *,***§§###	0.38±0.08 ***	76.23±4.77 ###
nt-neoSCs	1/8	0.02±0.02	0.03±0.03	96.79±3.21
tf-neoSCs-EV	1/8	0.01±0.01	0.06±0.06	97.92±2.08
tf-neoSCs-GDNF	0/8	na	na	na
tf-neoSCs-FGF-2^{18kDa}	0/8	na	na	na
13 weeks				
ANG	7/7	0.38±0.03 ***###	0.47±0.05 ***	50.39±4.66 ***###
nt-neoSCs	1/8	0.04±0.04	0.04±0.04	96.07±3.93
tf-neoSCs-EV	0/8	na	na	na
tf-neoSCs-GDNF	1/7	0.04±0.04	0.04±0.04	92.37±7.63
tf-neoSCs-FGF-2^{18kDa}	1/8	0.03±0.03	0.04±0.04	94.96±5.04
17 weeks				
ANG	7/7	0.61±0.03 ***	0.45±0.05 ***	8.52±9.43 ***
nt-neoSCs	1/7	0.06±0.06	0.04±0.04	92.99±7.01
tf-neoSCs-EV	0/6	na	na	na
tf-neoSCs-GDNF	1/7	0.04±0.04	0.03±0.03	91.36±8.64
tf-neoSCs-FGF-2^{18kDa}	4/7	0.15±0.06	0.25±0.05	71.78±10.74

Result from noninvasive electrodiagnostical evaluation at different time points after surgery. Data are given as mean±SEM. For statistical analyses, all animals were included, and in case of no signal detection, null values (amplitude ratio, NCV ratio) or 100% (AxL) were set. Noninvasive recordings from the tibialis anterior muscles revealed significant differences between the autologous nerve graft (ANG) group and all groups that were treated with either of the composite chitosan conduits. Additionally, sole treatment with the gold standard ANG led to a significant improvement of muscle reinnervation over time. Results were tested for significance ($p<0.05$) using two-way ANOVA, Tukey's multiple comparisons. *$p<0.05$, **$p<0.01$, ***$p<0.001$ versus values all fellow groups at the same time point; §§$p<0.01$ versus ANG 13 weeks; ###$p<0.001$ versus ANG 17 weeks. Abbreviations: na, not available; NCV, nerve conduction velocity; AxL, axon loss; ANG, autologous nerve graft; nt-neoSCs, nontransfected neonatal Schwann cells; tf-neoSCs, transfected neonatal Schwann cells; EV, empty vector; GDNF, glial cell line-derived neurotrophic factor; FGF-2^{18kDa}, fibroblast growth factor 2 (18 kDa isoform).

Table 2. Nerve Conduction Velocity, Axon Loss, and Recruited Axons as Calculated From the Plantar (PL) Muscle Recordings

	Animals per Group	Amplitude Ratio	NCV Ratio	AxL (%)
9 weeks				
ANG	6/8	0.07 ± 0.03 ###	0.29 ± 0.07 **,***§##	83.53 ± 9.79 ##
nt-neoSCs	0/8	na	na	na
tf-neoSCs-EV	0/7	na	na	na
tf-neoSCs-GDNF	0/5	na	na	na
tf-neoSCs-FGF-2^{18kDa}	0/6	na	na	na
13 weeks				
ANG	7/7	0.22 ± 0.06 *,**	0.54 ± 0.07 ***	74.25 ± 5.31
nt-neoSCs	1/8	0.02 ± 0.02	0.06 ± 0.06	97.37 ± 2.63
tf-neoSCs-EV	0/8	na	na	na
tf-neoSCs-GDNF	0/4	na	na	na
tf-neoSCs-FGF-2^{18kDa}	0/7	na	na	na
17 weeks				
ANG	7/7	0.34 ± 0.08 ***	0.57 ± 0.07 ***	46.31 ± 16.52 **,***
nt-neoSCs	1/7	0.07 ± 0.07	0.07 ± 0.07	92.83 ± 07.17
tf-neoSCs-EV	0/5	na	na	na
tf-neoSCs-GDNF	1/4	0.02 ± 0.02	0.07 ± 0.07	94.95 ± 5.05
tf-neoSCs-FGF-2^{18kDa}	1/6	0.05 ± 0.05	0.04 ± 0.04	91.67 ± 8.34

Results from noninvasive electrodiagnostical evaluation at different time points after surgery. Data are given as mean ± SEM. For statistical analyses, all animals were included, and in case of no signal detection, null values (amplitude ratio, NCV ratio) or 100% (AxL) were set. Recordings from the plantar muscles revealed that ANG treatment was superior in supporting motor recovery to all other experimental groups at each recording time point. Results were tested for significance ($p<0.05$) using two-way ANOVA, Tukey's multiple comparisons. *$p<0.05$, **$p<0.01$, ***$p<0.001$ versus values of all fellow groups at the same time point; §$p<0.05$, versus ANG 13 weeks; ##$p<0.01$, ###$p<0.001$ versus ANG 17 weeks. Abbreviations: na, not available; NCV, nerve conduction velocity; AxL, axon loss; ANG, autologous nerve graft; nt-neoSCs, nontransfected neonatal Schwann cells; tf-neoSCs, transfected neonatal Schwann cells; EV, empty vector; GDNF, glial cell line-derived neurotrophic factor; FGF-2^{18kDa}, fibroblast growth factor 2 (18 kDa isoform).

recordable from the TA muscle in four out of seven animals of the tf-neoSCs-FGF-2^{18kDa} group. One of these animals further displayed PL muscle reinnervation.

The data gained from the recordings were used to calculate the nerve conduction velocity (NCV) ratio, area under the curve (AUC), and amplitude ratio, with the latter two providing information with regard to functional axon loss (%) and an indication of number of conducting axons, respectively. Representatively the amplitude ratio results calculated from TA muscle CMAPs are illustrated in Figure 6 comparing the ANG and tf-neoSC-FGF-2^{18kDa} groups with continuous improvement of values. The ANG treatment enabled recovery of the amplitude size to almost 50% of contralateral control values at 17 weeks after surgery, while the tf-neoSCs-FGF-2^{18kDa} treatment supported recovery to 13% of control values. Regarding PL muscle reinnervation ANG treatment was superior to all treatments with composite nerve conduits (Table 2).

Calculations of NCV ratio and AUC, with estimation of the functional axon loss, supported the findings of the amplitude analysis. During noninvasive TA muscle recordings, animals of the ANG group showed significant faster NCVs and significantly lower loss of functional axons than animals of the experimental groups (Table 1).

In addition to the electrophysiological examination, the lower limb muscle weight ratio was determined upon sacrifice of the animals as another indicator for muscle reinnervation. As depicted in Figure 7, both the TA (Fig. 7A) and gastrocnemius (Fig. 7B) muscle weight ratio recovered in the tf-neoSCs-FGF-2^{18kDa} group to values no longer significantly different to the ANG group.

Macroscopic Analysis of the Reconstructed Nerves 17 Weeks After Surgery Indicated That NVR-Gel Might Have Impaired In Vivo Regeneration and That This Could Partly be Overcome by Suspension of tf-neoSCs-FGF-2^{18kDa} in It

After sacrifice of the animals (17 weeks after surgery), the reconstructed nerves were examined, and the results are listed in Table 3, and representative photographs are

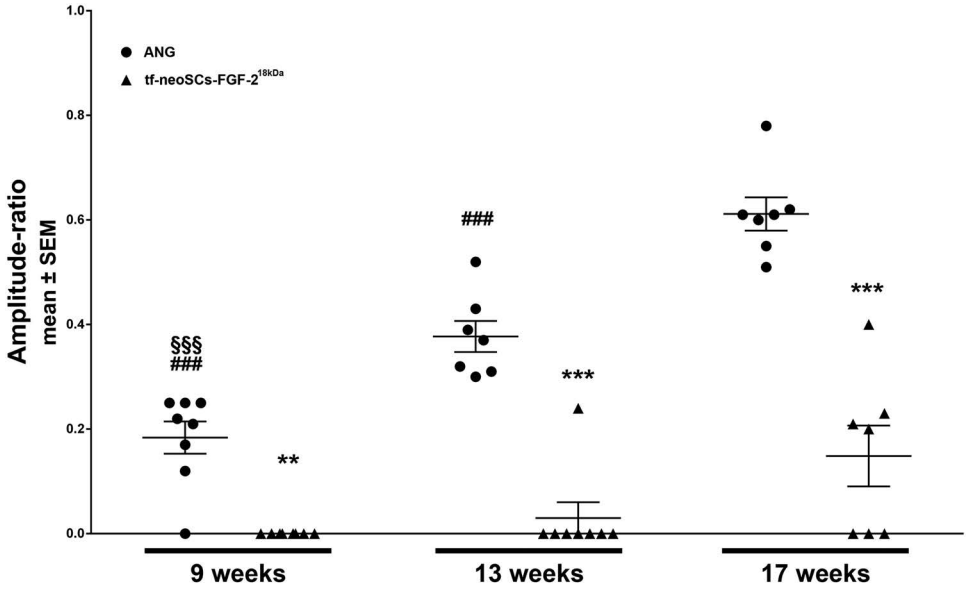

Figure 6. Results of the functional evaluation of motor recovery with electrophysiological assessment. Dot blot depicting the amplitude ratio calculated from noninvasive electrophysiological examination at different time points after surgery (mean ± SEM). Results were tested for significance ($p < 0.05$) using two-way ANOVA, Tukey's multiple comparisons. $^{**}p < 0.01$, $^{***}p < 0.001$ versus ANG group at the same time point; $^{###}p < 0.001$ versus ANG 17 weeks, §§§$p < 0.001$ versus ANG 13 weeks.

shown in Figure 8. While also from the functional test, all animals of the ANG group were considered as presenting regenerated sciatic nerves (Fig. 8A), exclusively suspension of tf-neoSCs-FGF-2^{18kDa} in the NVR-Gel used for composite chitosan nerve conduits resulted in substantial nerve tissue regeneration (Fig. 8B) in four out of seven animals (Table 3). In the tf-neoSCs-FGF-2^{18kDa} group, no complete failure of tissue regeneration was seen, but in the remaining three out of seven animals, only thin connections between the nerve ends were found. Substantial nerve tissue was only seen for single animals of the other experimental groups. Most of the composite nerve

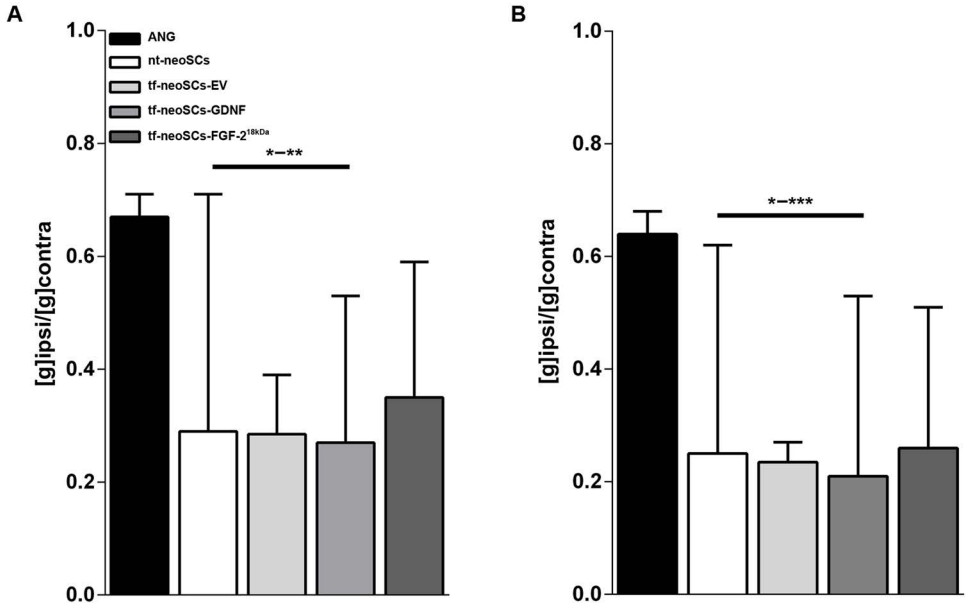

Figure 7. Results of the lower limb muscle weight analysis. Bar graphs illustrating the lower limb muscle weight ratio calculated upon sacrifice at 17 weeks after surgery for (A) the tibialis anterior and (B) the plantar muscles (median ± range). Results were tested for significance ($p < 0.05$) using Kruskal–Wallis test, Dunns multiple comparisons. $^{*}p < 0.05$, $^{**}p < 0.01$, $^{***}p < 0.001$ versus ANG.

Table 3. Macroscopically Detectable Regenerated Nerve Tissue Upon Explantation 17 Weeks After Surgery

	Animals/Group		
Group	Substantial Nerve Tissue	Thin Tissue Connection Between the Reconstructed Nerve Ends	No Recognizable Regeneration
ANG	7/7	0/7	0/7
nt-neoSCs	1/7	2/7	4/7
tf-neoSCs-EV	1/6	2/6	3/6
tf-neoSCs-GDNF	1/7	2/7	4/7
tf-neoSCs-FGF-2^{18kDa}	4/7	3/7	0/7

Inspection of the reconstructed sciatic nerves upon sacrifice of the animals revealed diverse numbers of animals per experimental group with substantial nerve regeneration, only thin connections between the nerve ends, or no recognizable tissue regeneration. Abbreviations: ANG, autologous nerve graft; nt-neoSCs, nontransfected neonatal Schwann cells; tf-neoSCs, transfected neonatal Schwann cells; EV, empty vector; GDNF, glial cell line-derived neurotrophic factor; FGF-2^{18kDa}, fibroblast growth factor 2 (18 kDa isoform).

conduits from the NVR-Gel alone group, the nt-neoSCs group, the tf-neoSCs-EV group, as well as the tf-neoSCs-GDNF group did not contain any recognizable nerve tissue but eventually a thin tissue connection between the reconstructed sciatic nerve ends (Fig. 8C).

Nerve Regeneration Through Composite Nerve Conduits Was Not Impaired by Inflammatory Reactions.

In order to analyze if modifying the hollow chitosan conduits into composite nerve conduits had an impact on the tissue reaction against the material, we histologically analyzed the connective tissue that has formed around the implanted nerve conduits as well as the nerve tissue within them. As an indicator for graft rejection, we first analyzed the number of multinuclear giant cells (MGCs) that had formed in it during the 17 weeks postoperative period (Fig. 9A, B). Only single MGCs were found in one out of four animals of the tf-neoSCs-EV group and in two out of six animals of the tf-neoSCs-FGF-2^{18kDa} group. Furthermore, no significant differences among the experimental groups were detectable with regard to the thickness (Fig. 9C) of the connective tissue as well as its area (Fig. 9D).

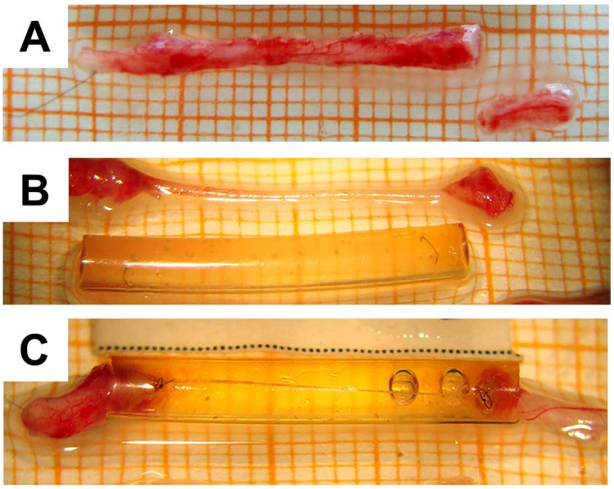

Figure 8. Representative photomicrographs of explanted specimens following a 4-month observation period. (A) Sciatic nerve regenerated through a 15-mm-reversed ANG. (B) Sciatic nerve substantially regenerated through a composite chitosan conduit filled with tf-neoSCs-FGF-2^{18kDa} suspended in NVR-Gel. (C) Sciatic nerve reconstructed with a composite chitosan conduit filled with tf-neoSCs-EV displaying only a thin connection between the bridged nerve ends. Specimens are placed on scale paper with 1-mm intersections.

Samples of substantial nerve tissue regeneration were subjected to ED1 (activated macrophages) staining and analyzed, but again no obvious differences among the samples from different groups were seen (data not shown).

Histological Analysis of Proximal Nerve Ends and Composite Nerve Conduits Displaying Failed Nerve Regeneration Demonstrated Impaired Axonal Regeneration Into Nerve Conduits That 17 Weeks After Surgery Still Contained Dense Hydrogel Residues in Their Lumen

Paraffin sections were obtained close to the proximal suture site connecting the composite nerve guide to the proximal nerve end as well as 1.5 mm more proximal within the proximal nerve end. Sections were double stained to detect activated macrophages (ED1) and axons (neurofilament 200 kDa, NF200). Again, no increased inflammatory reaction was detectable, but failed axonal regeneration was obvious as sections at the suture site did not or only contain few NF200 immunopositive axons entering the composite nerve conduits (Fig. 10A, B), while sections far more proximal contained visible amounts of axons (Fig. 10C, D).

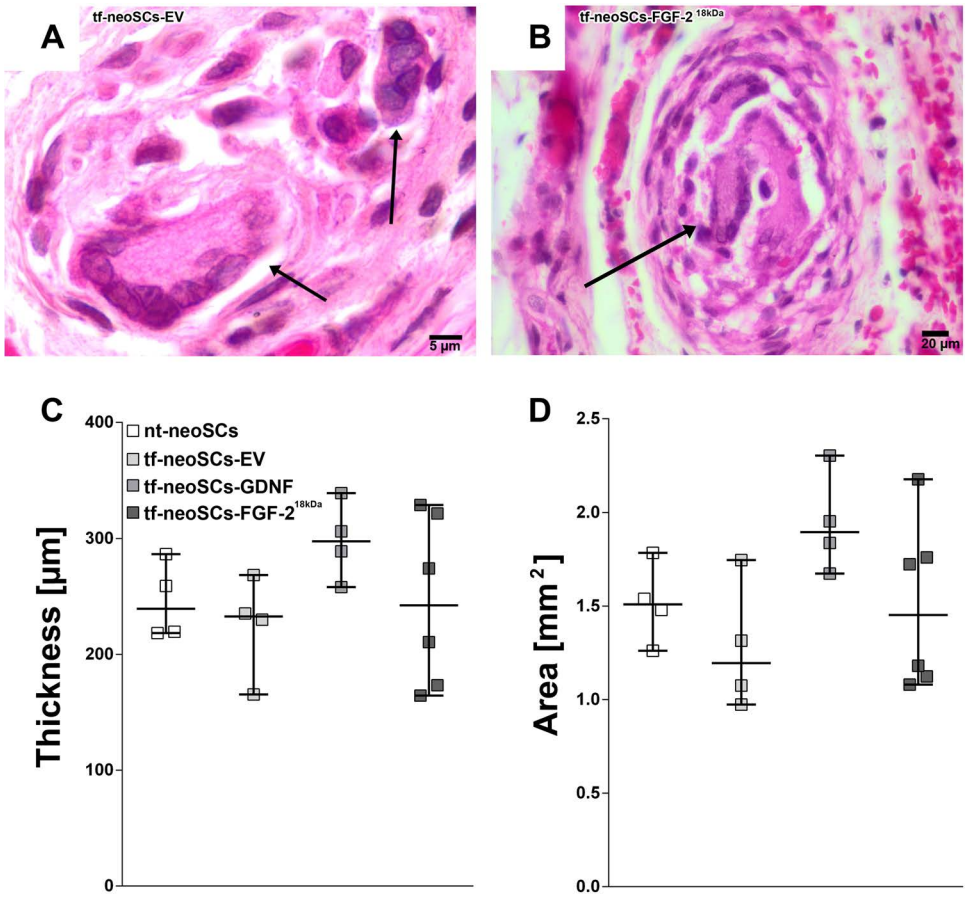

Figure 9. Results of the histological examination of the connective tissue formed around the composite nerve grafts. (A, B) Representative photomicrographs of single multinuclear giant cells that formed in the connective tissue that had developed around the composite nerve conduits. (C, D) Bar graphs illustrating the lack of significant differences between the experimental groups' connective tissue thickness (C) and area (D). Results were tested for significance ($p<0.05$) using Kruskal–Wallis test.

Morphometric Analysis of Distal Nerve Segments Revealed Differences in the Amount of Regenerated Myelinated Axons Between Autologous Nerve Grafting and Nerve Reconstruction With tf-neoSCs-FGF-2^{18kDa} Composite Nerve Conduits but no Differences in Axon Maturation and Myelination

The results of the morphometric analysis of all distal nerve segments originating from reconstructed nerves demonstrating functional recovery are listed in Table 4. As depicted in Figure 11, we compared the results obtained from the ANG group and the tf-neo-SCs-FGF-2^{18kDa} group with the data obtained from healthy nerves because only from those enough data were available for statistical analysis. Autologous nerve grafting resulted in total axon numbers significantly higher than in tf-neoSCs-FGF-2^{18lDa} or in healthy nerves distally to the injury site (Fig. 11A). Nerve fiber densities, however, were only significantly different between the regenerated nerves of the examined groups (Fig. 11A). In comparison to healthy axons, the mean axonal diameter, fiber diameter, and the myelin thickness were significantly reduced in the regenerated nerve segments (Fig. 11B). The g-ratio of axons regenerated in the tf-neoSCs-FGF-2^{18kDa} group was still significantly lower compared to healthy nerves, while that of regenerated axons in the ANG group did already recover to almost physiological levels (Fig. 11B). The distal nerve segment of the NVR-Gel alone group was processed for morphometrical analysis only, but again there were not enough samples with regenerating fibers to perform a statistical evaluation. Regenerating fibers within the distal nerve segments were only detectable in 1 out of 10 animals (Table 4). Furthermore, in three samples from this control group, few fibers were detectable in the periphery of the analyzed cross sections. Figure 12 shows high-resolution images of representative semithin sections, stained with Toluidine blue, of nerve samples regenerated through an ANG (A), a chitosan/NVR-Gel alone conduit (B), and a chitosan/NVR-Gel/tf-neoSCs-FGF-2^{18kDa} conduit (C). Regenerating fibers were detectable in the ANG group sample (A) and in the chitosan/NVR-Gel/tf-neoSC-FGF-2^{18kDa} sample (F),

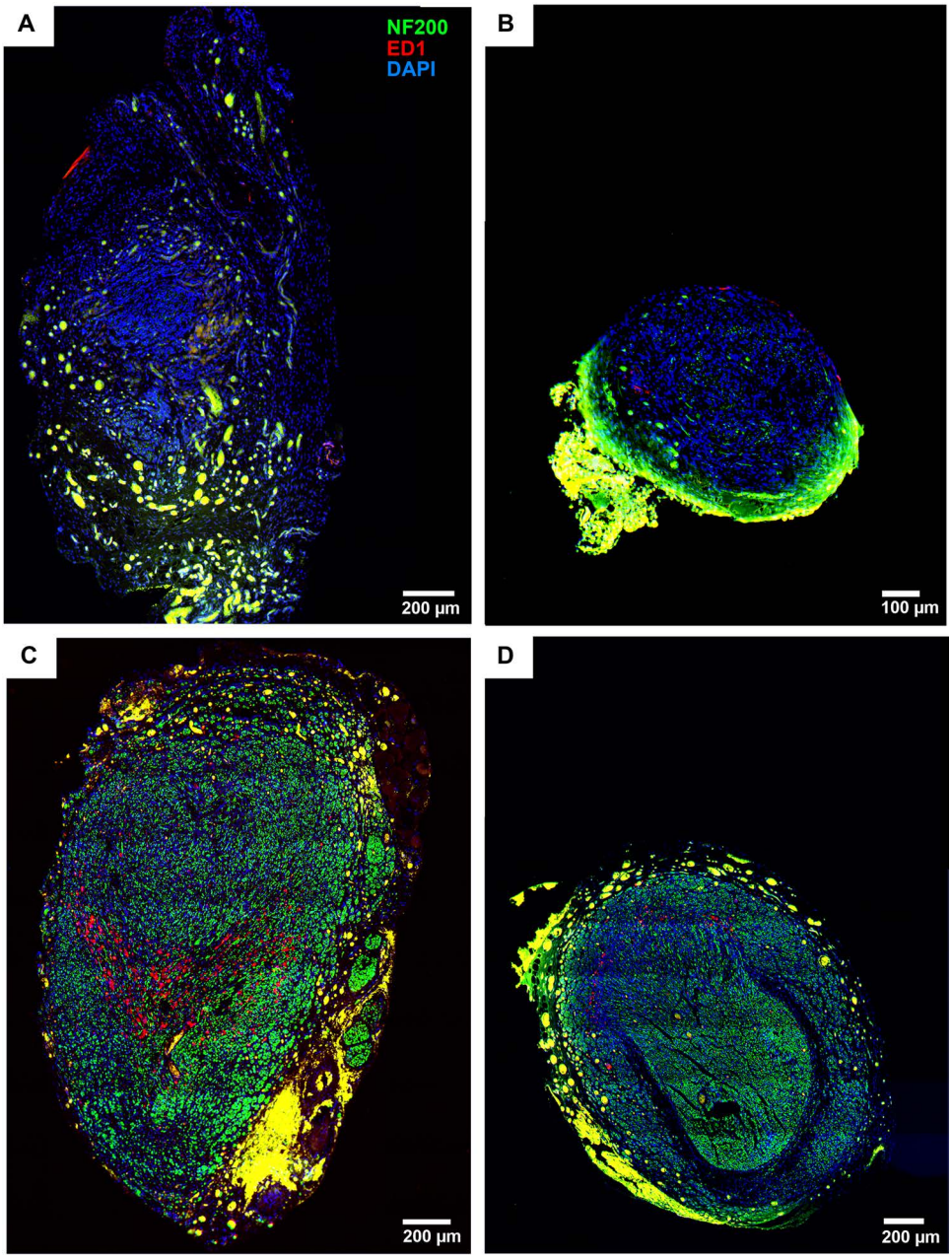

Figure 10. Results of the histological examination of nerve samples harvested proximal to the grafts. (A, B) Representative photomicrographs acquired from sections of proximal nerve stumps from which no or only few axons grew into the composite nerve conduits they have been connected to. (C, D) NF200 immunopositive axons were present only 1.5 mm proximal to the proximal suture sites of the same samples.

whereas in (B) a nerve sample from the NVR-Gel alone group, where fibers are regenerated in the outer periphery of the cross section, is presented.

DISCUSSION

Studies that address the treatment of long peripheral nerve defects have to take into account numerous variables that decide whether or not a conduit will successfully support peripheral axon regeneration. The clinical gold standard treatment for the reconstruction of long peripheral nerve defects is the use of autologous nerve tissue. The autologous nerve graft is therefore the proper control for preclinical animal studies evaluating peripheral nerve tissue engineering approaches (6). Because of the proregenerative properties provided by autologous nerve grafts also the functional outcome after nerve reconstruction can be adequately addressed

Table 4. Results of Analysis of the Nerve Morphometry of Distal Nerve Segments Originating From Nerves That Demonstrated Functional Recovery

Group	Animals per Group	Total Axon Number	Nerve Fiber Density (number/mm^2)	Axon Diameter (µm)	Fiber Diameter (µm)	Myelin Thickness (µm)	g-Ratio
Healthy nerve	10/10	8,796.67 ± 464.06	16,598.61 ± 595.05	4.64 ± 0.15	6.94 ± 0.17	1.15 ± 0.03	0.66 ± 0.01
ANG	7/7	11,294.64 ± 769.39	28,306.61 ± 1,610.38	2.15 ± 0.14	3.25 ± 0.19	0.55 ± 0.03	0.65 ± 0.01
NVR-Gel	1/10	8,844.75	17,660.68	2.39	3.67	0.64	0.62
nt-neoSCs	1/7	14,864	44,586	1.81	2.83	0.51	0.63
tf-neoSCs							
-EV	0/6	na	na	na	na	na	na
-GDNF	1/7	12,022	33,240	1.83	2.77	0.47	0.67
-FGF-2^{18kDa}	4/7	6,298.62 ± 1,868,64	20,927.33 ± 2,304.59	1.65 ± 0.03	2.72 ± 0.10	0.54 ± 0.04	0.60 ± 0.02

Data are given in mean ± SEM for ANG, tf-neoSCs-FGF-2^{18kDa}, and healthy nerve samples, while for single animals with functional recovery, the single values are presented. Abbreviations: na, not available; ANG, autologous nerve graft; NVR-Gel, chitosan conduits with solely NVR-Gel; nt-neoSCs, nontransfected neonatal Schwann cells; tf-neoSCs, transfected neonatal Schwann cells; EV, empty vector; GDNF, glial cell line-derived neurotrophic factor; FGF-2^{18kDa}, fibroblast growth factor 2 (18 kDa isoform).

in a comprehensive study design (6) as it has been chosen for the present investigation. We detected high degrees of functional motor recovery and almost complete recovery of mechanosensitivity in 100% of ANG group animals. High percentages of up to 100% of animals demonstrating functional recovery of the sciatic nerve after autologous nerve grafting is regularly reported from analyzing motor parameters like the animals' walking pattern, kinematic data, electrophysiological examination of lower limb or plantar muscles (5,20,34,35,39,46,56,69,70,77). Recovery of sensory functions, especially mechanosensitivity or nociception, is more often addressed in studies related to the development of neuropathic pain but usually also recovers to a great extent after autologous nerve grafting (41,46,58). Although the PNS has an intrinsic capacity to regenerate, problems like misdirection of axons, insufficient structural support of axonal outgrowth as well as deprivation from regeneration-promoting factors can limit the success rate especially across long gaps

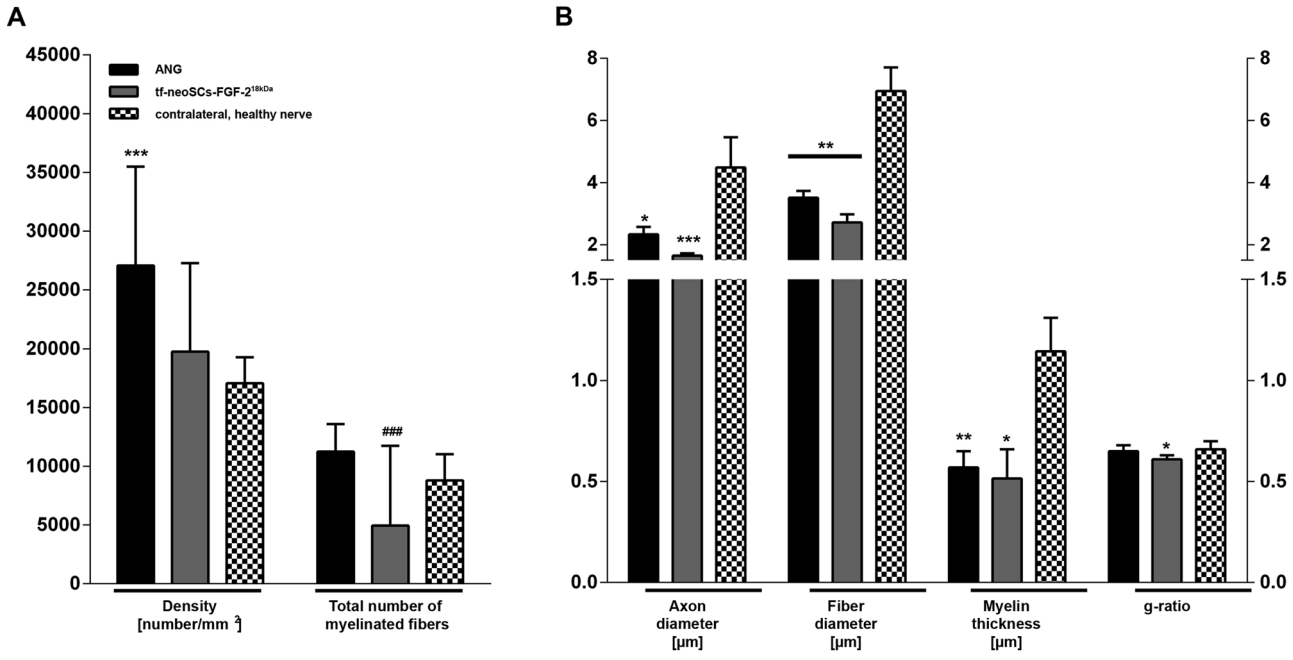

Figure 11. Results of the histological examination of nerve samples harvested distal to the grafts. Comparison of results obtained in morphometric analysis of distal nerve segments from the ANG and tf-neoSCs-FGF-2^{18kDa} groups. (A) Bar graphs depicting the comparison parameters related to the quantification of regenerated myelinated axons. (B) Bar graphs depicting parameters related to axonal maturation. Data are given in median ± range. Results were tested for significance ($p < 0.05$) using Kruskal–Wallis test, Dunn's multiple comparisons. *$p < 0.05$, **$p < 0.01$, ***$p < 0.001$ versus contralateral, healthy control values; ###$p < 0.001$ versus ANG.

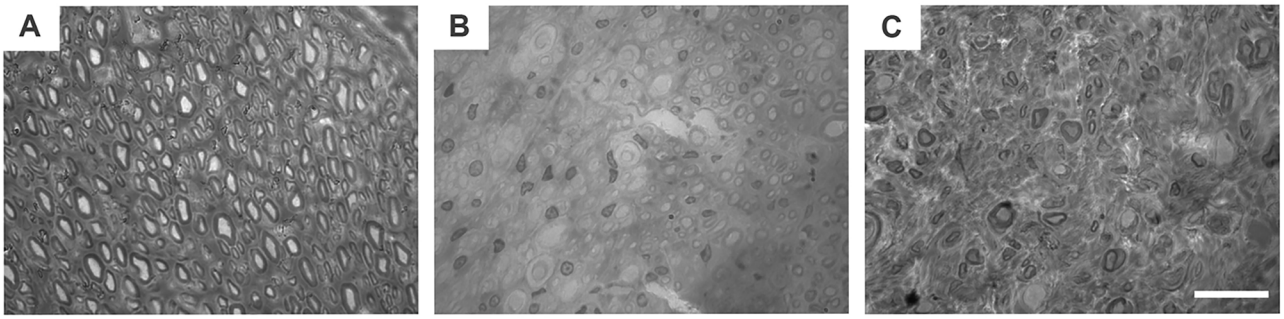

Figure 12. High-resolution images of representative semithin sections, stained with Toluidine blue, of distal nerve samples. Nerve samples were harvested after reconstruction with (A) an autologous nerve graft, (B) a chitosan/NVR-Gel alone conduit, (C) a chitosan/NVR-Gel/tf-neoSC-FGF-2^{18kDa} conduit. Particularly, nerve samples from the NVR-Gel alone group (B) demonstrated growth of regenerating fibers in the outer periphery of the cross sections. Scale bar: 20 µm.

(4,18,23,34,44). These impediments are the reason why also with autologous nerve grafting functional recovery is never complete (remains partial) in comparison to healthy control nerves. With regard to the structural support of axonal outgrowth intraluminal fillers such as different hydrogels are thought to be favorable, since they potentially support migration of host SCs together with axonal outgrowth (16). It has also been reported that neurotrophic factor free matrices filling the lumen of hollow nerve conduits result in poor regeneration, while the addition of specific neurotrophic factors generally mediates better regeneration properties than empty tubes (59).

In the current study, we therefore aimed at a combined approach of using composite nerve conduits composed of hollow chitosan tubes, which had already demonstrated nerve regeneration-supporting properties (23,34), filled with NVR-Gel. NVR-Gel as a luminal filler was supposed to provide a regenerative matrix for peripheral axons (65). For the in vivo application into nerve conduits, NVR-Gel was used in a concentration/density of 0.5%. This concentration allowed its secure injection into the nerve conduits without the risk of immediate efflux. Regeneration-promoting neurotrophic factors have been additionally delivered to the composite nerve conduits by genetically engineered SCs. Physiologically upon nerve transection, the local SCs dedifferentiate, start to proliferate, and to migrate to the injury site, where they support and guide regrowing axons to the distal targets (54). Consequently, transplantation of SCs within nerve conduits is thought to be advantageous and their genetic modification into neurotrophic factor delivery systems has proven to support axonal and functional recovery (32,48,59).

NVR-Gel Demonstrates a Discrepancy Between In Vitro and In Vivo Properties

The results seen in the current study clearly demonstrate that the viability of SCs suspended in 0.5% NVR-Gel and delivered into chitosan nerve conduits is not altered and that they develop their typical morphology and are able to migrate and to start alignment during their time in culture. Furthermore, in vitro 0.5% NVR-Gel allows neurite extension from PC-12 cells as well as dissociated DRG drop cultures. In previous studies, NVR-Gel did also demonstrate its favorable properties as a regenerative matrix in vitro (79), and it has been successfully used in spinal cord reconstruction in vivo (63). The mode of application of a hydrogel for spinal cord repair, however, differs from that for peripheral nerve reconstruction. Still, it was quite surprising to us that NVR-Gel as luminal filler in composite chitosan nerve conduits did not support axonal regeneration, when used for reconstruction of 15-mm rat sciatic nerve gaps. While hollow conduits did already result in a success rate of 57% motor recovery in the same model (23), regenerating fibers within the distal nerve segments were only detectable in 1 out of 10 animals when adding pure NVR-Gel as a luminal filler. Furthermore, in three samples from this control group, few fibers were detectable in the periphery of the analyzed cross sections. These results indicate that the NVR-Gel acted as a physical barrier to the regenerating axons. Since the same concentration/density of NVR-Gel was used in our in vitro and in vivo approaches, this finding suggests that NVR-Gel properties changed over time within chitosan composite nerve conduits and then impaired axonal outgrowth in vivo. Such secondary changes may have led to reduction of luminal space and reduced speed of NVR-Gel removal from the chitosan tubes. For a laminin-containing hydrogel, different from NVR-Gel, it was assumed by others that due to secondary swelling in vivo initially enhanced axonal regeneration was turned into its inhibition (49). We have to conclude that the hydrogel may have hampered nerve regeneration through the composite nerve conduits, although potentially supportive SCs have been suspended within it.

Transplantation of Genetically Modified Schwann Cells Is an Interesting Tool for Neurotrophic Factor Delivery

Indeed, we successfully demonstrated the survival of genetically modified tf-neoSCs in NVR-Gel-filled chitosan conduits, as well as their neurite inductive bioactivity in cultures of PC-12 cells and dissociated DRG drops in vitro. Therefore, the transplanted tf-neoSCs are not supposed to have impaired axonal regeneration through the composite nerve conduits. Furthermore, we did already demonstrate that SCs suspended in Matrigel™ support regeneration across rat sciatic nerve defects through silicone conduits (32,36). Also others have previously described that collagen nerve guidance conduits seeded with SCs enhance rat peripheral nerve regeneration (3,7,59). We additionally found no signs of composite nerve guide rejection such as massive formation of MGCs or increased tissue infiltration with activated macrophages. These results are in line with data previously obtained with hollow chitosan conduits and indicate that our composite nerve conduits have been biologically inert (23,34). Again we have to conclude that neither the chitosan nerve conduit itself nor the transplanted SCs have been an obstacle for regeneration. This conclusion is fostered by another study describing that also a chitosan/glycerol-β-phosphate disodium salt hydrogel-containing SCs injected into nerve conduits led to complete failure of regeneration (10-mm gap rat sciatic nerve gap), while SCs in suspension or culture medium alone allowed regeneration (78).

tf-neoSCs-FGF-2^{18kDa} Support Partial Functional Recovery Through Composite Nerve Conduits

In addition to the formation of regenerative tissue and axonal regeneration, peripheral nerve reconstruction should result in functional recovery. With regard to the time course and the extent of functional recovery, all composite nerve conduits have to compete with the gold standard of autologous nerve grafting, which was in the current study represented by the ANG group. We mainly evaluated the mechanical pain threshold as indicator for sensory recovery, and electrophysiological parameters were assessed as a measure for motor recovery. Owing to the fact that only in the tf-neoSCs-FGF-2^{18kDa} group functional nerve regeneration occurred in animal numbers high enough for statistical comparison to the ANG group, the differences between these two groups will be discussed in the following.

Altogether, the obtained results demonstrate the initial full sensory denervation of the lateral plantar paw for up to a minimum of 4 weeks after nerve injury. Under healthy conditions, tibial and sural branches of the sciatic nerve as well as the saphenous nerve provide sensory innervation to the medial paw site, while the plantar lateral area is exclusively innervated by branches of the sciatic nerve (14). In all animals of the ANG group (100%), return of sensation was seen after a time period of 9 weeks, when the response could already be detected upon light stimulation representing hyperalgesia. In a similar manner, 40% of the animals of the tf-neoSCs-FGF-2^{18kDa} group showed signs of sensory recovery. Based on experiments that included cutting of the saphenous nerve at the end of the observation period (not performed in the current study) the hypersensitivity in the lateral paw site can be attributed to the arrival of regenerating axons to this territory (15). Comparing ANG treatment to nerve reconstruction with tf-neoSCs-FGF-2^{18kDa} composite nerve conduits clearly indicates that regrowth of sensory fibers is supported to a greater extent by autologous nerve grafting.

Motor recovery was analyzed by means of electrophysiological examination at different time points after surgery. Similar to the findings related to sensory recovery, reinnervation of distal muscle targets and subsequent motor recovery was seen for all animals, which had received ANGs (100%) for nerve reconstruction and for 57% of the animals of the tf-neoSCs-FGF-2^{18kDa} group. Analysis of the lower hindlimb muscle weight ratios further indicated progressing reduction of muscle atrophy attributable to muscle reinnervation. The fact that motor recovery after transplantation of tf-neoSCs-FGF-2^{18kDa} is ahead of sensory recovery is in accordance with our previous experiences (32) and to reports from in vitro studies describing more pronounced effects of FGF-2^{18kDa} on motor than on sensory neurite outgrowth (2). This distinguishable in vitro effect is also illustrated by our report of a strong neurite inducing effect of tf-neoSCs-FGF-2^{18kDa} in the PC12 cell assay and only a minimal effect in the DRG neurite outgrowth assay. Furthermore, the ANG is the standard therapy for bridging critical length sciatic nerve defects in the rat model and for this best and most complete sensory as well as motor recovery, as detected also in the current study, can be expected (23). Transplantation of all other neoSC types did mainly result in failure of regeneration. We attribute this failure to mechanical impairments that possibly developed due to the secondary changes of NVR-Gel properties in vivo as discussed above.

Factors Contributing to Incomplete Motor Recovery After Tubular Nerve Repair

No definite solution for incomplete functional recovery has been found so far. It is well established that topographical peripheral motor and sensory projections of mixed nerves, for example, the sciatic nerve, are distorted during the regeneration process and that this hampers full functional recovery especially over long nerve gaps (71,72). Structuring the lumen of tubular nerve conduits, for example, with hydrogels like in the current study, is thought to minimize this distortion. Furthermore, specific neurotrophic support of motor neurons and their regrowing axons, like, for example, with GDNF or FGF-2^{18kDa}, has been established to induce preferential motor

reinnervation and to reduce growth of regenerating motor axons along sensory tracts (50). Within the target tissue, however, another obstacle to valid functional recovery can occur, which has been described as polyinnervation of neuromuscular junctions (66). Interestingly, it has been shown that endogenous expression of FGF-2^{18kDa} plays a critical role in limiting polyinnervation, as in mice lacking FGF-2^{18kDa} expression, polyinnervation was described to be higher and related to decreased functional recovery of the facial nerve after lesion and repair in comparison to wild-type mice (64). The impact of polyinnervation of neuromuscular endplates on the outcome of functional motor recovery in the sciatic nerve model in rats is not yet investigated in detail. From the rat facial nerve model, however, some interesting adjunct attempts emerged that could also be helpful in the context of limb recovery, like, for example, the stabilization of microtubule assembly within the regenerating nerve (24).

Differential Effects of Overexpressed FGF-2^{18kDa} and GDNF Within Composite Nerve Conduits

In the current study, the delivery of FGF-2^{18kDa} helped to overcome the shortcomings of the composite nerve conduits, while delivery of GDNF did not. One reason for this difference could be linked to the behavior of the neurotrophic factor overexpressing cells within the conduits. For tf-neoSCs-FGF-2^{18kDa}, we detected a higher metabolic activity after 24 h within the chitosan conduits than for tf-neoSCs-GDNF. Although the difference in metabolic activity was not significant, this indicates that tf-neoSCs-FGF-2 were more intensively interacting with the NVR-Gel and thereby eventually loosening the gel structure or simply populating it in a more homogenous way. In the following, it may have been easier for regenerating axons or host Schwann cells to enter the composite chitosan conduits. Still, the missing effect of GDNF was unexpected, since, for example, Patel et al. (58) could show that GDNF and laminin-blended chitosan conduits enhanced functional and sensory peripheral nerve functional recovery across 10-mm gaps in rats. Also Kokai and colleagues (45) reported functional recovery across a long gap (15 mm), when delivering GDNF to the lesion site via microspheres. However, the failure of tf-neoSCs-GDNF to support regeneration through composite nerve conduits in the current study underscores another hypothesis, namely that this factor may be especially effective in case of delayed repair and fails to promote regeneration when administered immediately after nerve transection (10,11,37,74,75).

The specific support of functional recovery after immediate nerve reconstruction with transplantation of tf-neoSCs-FGF-2^{18kDa} into composite nerve conduits, however, could have been expected based on previous experiences. It has been demonstrated that FGF-2^{18kDa} promotes neurite outgrowth from spinal motoneurons in vitro (2) as well as axonal elongation and myelination in vivo (68). Additionally, we showed before that FGF-2^{18kDa} delivered by tf-neoSCs into silicone tubes predominately supports motor recovery across rat sciatic nerve defects (32,33). In conclusion, tf-neoSCs-FGF-2^{18kDa} incorporated into composite nerve conduits support peripheral nerve regeneration in general and motor recovery in particular. This may not only be attributed to specific action of the delivered protein on motor axons but also on its effect on the local host SCs in the bridged nerve ends. Transgenic mice overexpressing FGF-2 displayed an increased number of proliferating SCs as well as more axons 1 week after nerve crush (42). An increased SC migration due to locally increased levels of FGF-2^{18kDa} may have been the basis for increased axonal growth into the tf-neoSCs-FGF-2^{18kDa} composite nerve conduits and subsequent functional recovery in the current study.

CONCLUSION AND PERSPECTIVE

We demonstrate here that genetic engineering of SCs is a valuable tool for peripheral nerve tissue engineering. Especially FGF-2^{18kDa} delivery by these cells is able to increase functional recovery through composite nerve conduits. We further have to realize that 0.5% NVR-Gel is an optimal matrix to analyze peripheral nerve regeneration in vitro but does in its current composition not guarantee for the same in vivo. Further attempts are needed to optimize composite chitosan nerve conduits in order to provide structural support as well as cell-based drug delivery systems for long nerve gap repair. As the main components of NVR-Gel (hyaluronic acid and laminin) are known to potentially support peripheral nerve regeneration, modifications of the gel would be an option to improve its performance. Handling of a more soluble NVR-Gel, however, demonstrated the risk of sudden leakage of the NVR-Gel and minimized standardization of the composite nerve conduits. Consequently, standardized and controlled cell delivery would no longer be possible. Therefore, conversion of the NVR-Gel into a solid state, for example, by freeze drying, seems to be intriguing. Once this has been established also cell delivery protocols to these modified composite nerve conduits can be established and investigated in future in vivo attempts.

ACKNOWLEDGMENTS: Medical-grade chitosan for manufacturing the chitosan conduits was supplied by Altakitin SA (Lisbon, Portugal). The authors thank Dr. Andreas Ratzka, Institute of Neuroanatomy, for the construction of the plasmids used in this study. We are further thankful to Silke Fischer, Natascha Heidrich, Kerstin Kuhlemann, Jennifer Metzen, Hildegard Streich, Maike Wesemann, and Natalie Schecker (all from the Institute of Neuroanatomy, Hannover Medical School) for their technical support. This study was supported by the European Community's Seventh Framework Programme (FP7-HEALTH-2011) under grant agreement No. 278612 (BIOHYBRID). The authors declare no conflicts of interest.

REFERENCES

1. Aebischer, P.; Guenard, V.; Brace, S. Peripheral nerve regeneration through blind-ended semipermeable guidance channels: Effect of the molecular weight cutoff. J. Neurosci. 9(10):3590–3595; 1989.
2. Allodi, I.; Casals-Diaz, L.; Santos-Nogueira, E.; Gonzalez-Perez, F.; Navarro, X.; Udina, E. FGF-2 low molecular weight selectively promotes neuritogenesis of motor neurons in vitro. Mol. Neurobiol. 47(2):770–781; 2013.
3. Allodi, I.; Mecollari, V.; Gonzalez-Perez, F.; Eggers, R.; Hoyng, S.; Verhaagen, J.; Navarro, X.; Udina, E. Schwann cells transduced with a lentiviral vector encoding Fgf-2 promote motor neuron regeneration following sciatic nerve injury. Glia 62(10):1736–1746; 2014.
4. Allodi, I.; Udina, E.; Navarro, X. Specificity of peripheral nerve regeneration: Interactions at the axon level. Prog. Neurobiol. 98(1):16–37; 2012.
5. Alluin, O.; Wittmann, C.; Marqueste, T.; Chabas, J. F.; Garcia, S.; Lavaut, M. N.; Guinard, D.; Feron, F.; Decherchi, P. Functional recovery after peripheral nerve injury and implantation of a collagen guide. Biomaterials 30(3):363–373; 2009.
6. Angius, D.; Wang, H.; Spinner, R. J.; Gutierrez-Cotto, Y.; Yaszemski, M. J.; Windebank, A. J. A systematic review of animal models used to study nerve regeneration in tissue-engineered scaffolds. Biomaterials 33(32):8034–8039; 2012.
7. Ansselin, A. D.; Fink, T.; Davey, D. F. Peripheral nerve regeneration through nerve guides seeded with adult Schwann cells. Neuropathol. Appl. Neurobiol. 23(5):387–398; 1997.
8. Apel, P. J.; Garrett, J. P.; Sierpinski, P.; Ma, J.; Atala, A.; Smith, T. L.; Koman, L. A.; Van Dyke, M. E. Peripheral nerve regeneration using a keratin-based scaffold: Long-term functional and histological outcomes in a mouse model. J. Hand Surg. Am. 33(9):1541–1547; 2008.
9. Bell, J. H.; Haycock, J. W. Next generation nerve guides: Materials, fabrication, growth factors, and cell delivery. Tissue Eng. Part B Rev. 18(2):116–128; 2012.
10. Boyd, J. G.; Gordon, T. Glial cell line-derived neurotrophic factor and brain-derived neurotrophic factor sustain the axonal regeneration of chronically axotomized motoneurons in vivo. Exp. Neurol. 183(2):610–619; 2003.
11. Boyd, J. G.; Gordon, T. Neurotrophic factors and their receptors in axonal regeneration and functional recovery after peripheral nerve injury. Mol. Neurobiol. 27(3):277–324; 2003.
12. Bozkurt, A.; Boecker, A.; Van Neerven, S.; O'Dey, D. M.; Oplander, C.; Brook, G.; Pallua, N. A flexible, sterile, and cost-effective retractor system for microsurgery. Microsurgery 31(8):668–670; 2011.
13. Bozkurt, A.; Lassner, F.; O'Dey, D.; Deumens, R.; Bocker, A.; Schwendt, T.; Janzen, C.; Suschek, C. V.; Tolba, R.; Kobayashi, E.; Sellhaus, B.; Tholl, S.; Eummelen, L.; Schugner, F.; Damink, L. O.; Weis, J.; Brook, G. A.; Pallua, N. The role of microstructured and interconnected pore channels in a collagen-based nerve guide on axonal regeneration in peripheral nerves. Biomaterials 33(5):1363–1375; 2012.
14. Cobianchi, S.; Casals-Diaz, L.; Jaramillo, J.; Navarro, X. Differential effects of activity dependent treatments on axonal regeneration and neuropathic pain after peripheral nerve injury. Exp. Neurol. 240:157–167; 2013.
15. Cobianchi, S.; de Cruz, J.; Navarro, X. Assessment of sensory thresholds and nociceptive fiber growth after sciatic nerve injury reveals the differential contribution of collateral reinnervation and nerve regeneration to neuropathic pain. Exp. Neurol. 255:1–11; 2014.
16. Daly, W.; Yao, L.; Zeugolis, D.; Windebank, A.; Pandit, A. A biomaterials approach to peripheral nerve regeneration: Bridging the peripheral nerve gap and enhancing functional recovery. J.R. Soc. Interface 9(67):202–221; 2012.
17. de Ruiter, G. C.; Malessy, M. J.; Yaszemski, M. J.; Windebank, A. J.; Spinner, R. J. Designing ideal conduits for peripheral nerve repair. Neurosurg. Focus 26(2):E5; 2009.
18. de Ruiter, G. C.; Spinner, R. J.; Malessy, M. J.; Moore, M. J.; Sorenson, E. J.; Currier, B. L.; Yaszemski, M. J.; Windebank, A. J. Accuracy of motor axon regeneration across autograft, single-lumen, and multichannel poly(lactic-co-glycolic acid) nerve tubes. Neurosurgery 63(1):144–153; discussion 153–155; 2008.
19. Deumens, R.; Bozkurt, A.; Meek, M. F.; Marcus, M. A.; Joosten, E. A.; Weis, J.; Brook, G. A. Repairing injured peripheral nerves: Bridging the gap. Prog. Neurobiol. 92(3):245–276; 2010.
20. di Summa, P. G.; Kalbermatten, D. F.; Pralong, E.; Raffoul, W.; Kingham, P. J.; Terenghi, G. Long-term in vivo regeneration of peripheral nerves through bioengineered nerve grafts. Neuroscience 181:278–291; 2011.
21. Fex Svennigsen, A.; Dahlin, L. B. Repair of the peripheral nerve-remyelination that works. Brain Sci. 3(3):1182–1197; 2013.
22. Geuna, S. Appreciating the difference between design-based and model-based sampling strategies in quantitative morphology of the nervous system. J. Comp. Neurol. 427(3):333–339; 2000.
23. Gonzalez-Perez, F.; Cobianchi, S.; Geuna, S.; Barwig, C.; Freier, T.; Udina, E.; Navarro, X. Tubulization with chitosan guides for the repair of long gap peripheral nerve injury in the rat. Microsurgery 35(4):300–308; 2015.
24. Grosheva, M.; Guntinas-Lichius, O.; Angelova, S. K.; Kuerten, S.; Alvanou, A.; Streppel, M.; Skouras, E.; Sinis, N.; Pavlov, S.; Angelov, D. N. Local stabilization of microtubule assembly improves recovery of facial nerve function after repair. Exp. Neurol. 209(1):131–144; 2008.
25. Grothe, C.; Jungnickel, J.; Haastert, K. Physiological role of basic FGF in peripheral nerve development and regeneration: Potential for reconstruction approaches. Future Neurol. 3(5):605–612; 2008.
26. Grothe, C.; Meisinger, C.; Claus, P. In vivo expression and localization of the fibroblast growth factor system in the intact and lesioned rat peripheral nerve and spinal ganglia. J. Comp. Neurol. 434(3):342–357; 2001.
27. Grothe, C.; Meisinger, C.; Holzschuh, J.; Wewetzer, K.; Cattini, P. Over-expression of the 18 kD and 21/23 kD fibroblast growth factor-2 isoforms in PC12 cells and Schwann cells results in altered cell morphology and growth. Brain Res. Mol. Brain Res 57(1):97–105; 1998.
28. Grothe, C.; Nikkhah, G. The role of basic fibroblast growth factor in peripheral nerve regeneration. Anat. Embryol. (Berl) 204(3):171–177; 2001.
29. Gu, X.; Ding, F.; Yang, Y.; Liu, J. Construction of tissue engineered nerve grafts and their application in peripheral nerve regeneration. Prog. Neurobiol. 93(2):204–230; 2011.
30. Haastert, K.; Grosskreutz, J.; Jaeckel, M.; Laderer, C.; Bufler, J.; Grothe, C.; Claus, P. Rat embryonic motoneurons in long-term co-culture with Schwann cells-A system to investigate motoneuron diseases on a cellular level in vitro. J. Neurosci. Methods 142(2):275–284; 2005.

31. Haastert, K.; Grothe, C. Gene therapy in peripheral nerve reconstruction approaches. Curr. Gene Ther. 7(3):221–228; 2007.
32. Haastert, K.; Lipokatic, E.; Fischer, M.; Timmer, M.; Grothe, C. Differentially promoted peripheral nerve regeneration by grafted Schwann cells over-expressing different FGF-2 isoforms. Neurobiol. Dis. 21(1):138–153; 2006.
33. Haastert, K.; Ying, Z.; Grothe, C.; Gomez-Pinilla, F. The effects of FGF-2 gene therapy combined with voluntary exercise on axonal regeneration across peripheral nerve gaps. Neurosci. Lett. 443(3):179–183; 2008.
34. Haastert-Talini, K.; Geuna, S.; Dahlin, L. B.; Meyer, C.; Stenberg, L.; Freier, T.; Heimann, C.; Barwig, C.; Pinto, L. F.; Raimondo, S.; Gambarotta, G.; Samy, S. R.; Sousa, N.; Salgado, A. J.; Ratzka, A.; Wrobel, S.; Grothe, C. Chitosan tubes of varying degrees of acetylation for bridging peripheral nerve defects. Biomaterials 34(38):9886–9904; 2013.
35. Haastert-Talini, K.; Schaper-Rinkel, J.; Schmitte, R.; Bastian, R.; Muhlenhoff, M.; Schwarzer, D.; Draeger, G.; Su, Y.; Scheper, T.; Gerardy-Schahn, R.; Grothe, C. In vivo evaluation of polysialic acid as part of tissue-engineered nerve transplants. Tissue Eng. Part A 16(10):3085–3098; 2010.
36. Haastert-Talini, K.; Schmitte, R.; Korte, N.; Klode, D.; Ratzka, A.; Grothe, C. Electrical stimulation accelerates axonal and functional peripheral nerve regeneration across long gaps. J. Neurotrauma 28(4):661–674; 2011.
37. Hoke, A.; Gordon, T.; Zochodne, D. W.; Sulaiman, O. A. A decline in glial cell-line-derived neurotrophic factor expression is associated with impaired regeneration after long-term Schwann cell denervation. Exp. Neurol. 173(1):77–85; 2002.
38. Hoke, A.; Ho, T.; Crawford, T. O.; LeBel, C.; Hilt, D.; Griffin, J. W. Glial cell line-derived neurotrophic factor alters axon Schwann cell units and promotes myelination in unmyelinated nerve fibers. J. Neurosci. 23(2):561–567; 2003.
39. Huang, J.; Hu, X.; Lu, L.; Ye, Z.; Wang, Y.; Luo, Z. Electrical stimulation accelerates motor functional recovery in autograft-repaired 10 mm femoral nerve gap in rats. J. Neurotrauma 26(10):1805–1813; 2009.
40. Huelsenbeck, S. C.; Rohrbeck, A.; Handreck, A.; Hellmich, G.; Kiaei, E.; Roettinger, I.; Grothe, C.; Just, I.; Haastert-Talini, K. C3 Peptide promotes axonal regeneration and functional motor recovery after peripheral nerve injury. Neurotherapeutics 9(1):185–198; 2012.
41. Jin, J.; Limburg, S.; Joshi, S. K.; Landman, R.; Park, M.; Zhang, Q.; Kim, H. T.; Kuo, A. C. Peripheral nerve repair in rats using composite hydrogel-filled aligned nanofiber conduits with incorporated nerve growth factor. Tissue Eng. Part A 19(19–20):2138–2146; 2013.
42. Jungnickel, J.; Haase, K.; Konitzer, J.; Timmer, M.; Grothe, C. Faster nerve regeneration after sciatic nerve injury in mice over-expressing basic fibroblast growth factor. J. Neurobiol. 66(9):940–948; 2006.
43. Kehoe, S.; Zhang, X. F.; Boyd, D. FDA approved guidance conduits and wraps for peripheral nerve injury: A review of materials and efficacy. Injury 43(5):553–572; 2012.
44. Klimaschewski, L.; Hausott, B.; Angelov, D. N. The pros and cons of growth factors and cytokines in peripheral axon regeneration. Int. Rev. Neurobiol. 108:137–171; 2013.
45. Kokai, L. E.; Bourbeau, D.; Weber, D.; McAtee, J.; Marra, K. G. Sustained growth factor delivery promotes axonal regeneration in long gap peripheral nerve repair. Tissue Eng. Part A 17(9–10):1263–1275; 2011.
46. Korte, N.; Schenk, H. C.; Grothe, C.; Tipold, A.; Haastert-Talini, K. Evaluation of periodic electrodiagnostic measurements to monitor motor recovery after different peripheral nerve lesions in the rat. Muscle Nerve 44(1):63–73; 2011.
47. Lonka-Nevalaita, L.; Lume, M.; Leppanen, S.; Jokitalo, E.; Peranen, J.; Saarma, M. Characterization of the intracellular localization, processing, and secretion of two glial cell line-derived neurotrophic factor splice isoforms. J. Neurosci. 30(34):11403–11413; 2010.
48. Madduri, S.; Gander, B. Schwann cell delivery of neurotrophic factors for peripheral nerve regeneration. J. Peripher. Nerv. Syst. 15(2):93–103; 2010.
49. Madison, R. D.; da Silva, C.; Dikkes, P.; Sidman, R. L.; Chiu, T. H. Peripheral nerve regeneration with entubulation repair: Comparison of biodegradeable nerve guides versus polyethylene tubes and the effects of a laminin-containing gel. Exp. Neurol. 95(2):378–390; 1987.
50. Madison, R. D.; Robinson, G. A.; Chadaram, S. R. The specificity of motor neurone regeneration (preferential reinnervation). Acta Physiol. (Oxf) 189(2):201–206; 2007.
51. Mason, M. R.; Tannemaat, M. R.; Malessy, M. J.; Verhaagen, J. Gene therapy for the peripheral nervous system: A strategy to repair the injured nerve? Curr. Gene Ther. 11(2):75–89; 2011.
52. Meisinger, C.; Grothe, C. Differential regulation of fibroblast growth factor (FGF)-2 and FGF receptor 1 mRNAs and FGF-2 isoforms in spinal ganglia and sciatic nerve after peripheral nerve lesion. J. Neurochem. 68(3):1150–1158; 1997.
53. Morano, M.; Wrobel, S.; Fregnan, F.; Ziv-Polat, O.; Shahar, A.; Ratzka, A.; Grothe, C.; Geuna, S.; Haastert-Talini, K. Nanotechnology versus stem cell engineering: In vitro comparison of neurite inductive potentials. Int. J. Nanomedicine 9:5289–5306; 2014.
54. Muller, H. W.; Stoll, G. Nerve injury and regeneration: Basic insights and therapeutic interventions. Curr. Opin. Neurol. 11(5):557–562; 1998.
55. Navarro, X.; Buti, M.; Verdu, E. Autotomy prevention by amitriptyline after peripheral nerve section in different strains of mice. Restor. Neurol. Neurosci. 6(2):151–157; 1994.
56. Navarro, X.; Udina, E.; Ceballos, D.; Gold, B. G. Effects of FK506 on nerve regeneration and reinnervation after graft or tube repair of long nerve gaps. Muscle Nerve 24(7):905–915; 2001.
57. Niwa, H.; Yamamura, K.; Miyazaki, J. Efficient selection for high-expression transfectants with a novel eukaryotic vector. Gene 108(2):193–199; 1991.
58. Patel, M.; Mao, L.; Wu, B.; Vandevord, P. J. GDNF-chitosan blended nerve guides: A functional study. J. Tissue Eng. Regen. Med. 1(5):360–367; 2007.
59. Pfister, L. A.; Papaloizos, M.; Merkle, H. P.; Gander, B. Nerve conduits and growth factor delivery in peripheral nerve repair. J. Peripher. Nerv. Syst. 12(2):65–82; 2007.
60. Piccinini, E.; Kalkkinen, N.; Saarma, M.; Runeberg-Roos, P. Glial cell line-derived neurotrophic factor: Characterization of mammalian posttranslational modifications. Ann. Med. 45(1):66–73; 2013.
61. Ratzka, A.; Baron, O.; Grothe, C. FGF-2 deficiency does not influence FGF ligand and receptor expression during development of the nigrostriatal system. PLoS One 6(8):e23564; 2011.
62. Ratzka, A.; Kalve, I.; Ozer, M.; Nobre, A.; Wesemann, M.; Jungnickel, J.; Koster-Patzlaff, C.; Baron, O.; Grothe,

C. The colayer method as an efficient way to genetically modify mesencephalic progenitor cells transplanted into 6-OHDA rat model of Parkinson's disease. Cell Transplant. 21(4):749–762; 2012.
63. Rochkind, S.; Shahar, A.; Fliss, D.; El-Ani, D.; Astachov, L.; Hayon, T.; Alon, M.; Zamostiano, R.; Ayalon, O.; Biton, I. E.; Cohen, Y.; Halperin, R.; Schneider, D.; Oron, A.; Nevo, Z. Development of a tissue-engineered composite implant for treating traumatic paraplegia in rats. Eur. Spine J. 15(2):234–245; 2006.
64. Seitz, M.; Grosheva, M.; Skouras, E.; Angelova, S. K.; Ankerne, J.; Jungnickel, J.; Grothe, C.; Klimaschewski, L.; Hubbers, C. U.; Dunlop, S. A.; Angelov, D. N. Poor functional recovery and muscle polyinnervation after facial nerve injury in fibroblast growth factor-2-/- mice can be improved by manual stimulation of denervated vibrissal muscles. Neuroscience 182:241–247; 2011.
65. Shahar, A.; Nevo, Z.; Rochkind, S. Cross-linked hyaluronic acid-laminin gels and use thereof in cell culture and medical implants. Patent: PCT/IL2001/001050; USA; 2001.
66. Skouras, E.; Ozsoy, U.; Sarikcioglu, L.; Angelov, D. N. Intrinsic and therapeutic factors determining the recovery of motor function after peripheral nerve transection. Ann. Anat. 193(4):286–303; 2011.
67. Sun, X. L.; Chen, B. Y.; Duan, L.; Xia, Y.; Luo, Z. J.; Wang, J. J.; Rao, Z. R.; Chen, L. W. The proform of glia cell line-derived neurotrophic factor: A potentially biologically active protein. Mol. Neurobiol. 49(1):234–250; 2014.
68. Timmer, M.; Robben, S.; Muller-Ostermeyer, F.; Nikkhah, G.; Grothe, C. Axonal regeneration across long gaps in silicone chambers filled with Schwann cells overexpressing high molecular weight FGF-2. Cell Transplant. 12(3):265–277; 2003.
69. Udina, E.; Gold, B. G.; Navarro, X. Comparison of continuous and discontinuous FK506 administration on autograft or allograft repair of sciatic nerve resection. Muscle Nerve 29(6):812–822; 2004.
70. Valero-Cabre, A.; Navarro, X. H reflex restitution and facilitation after different types of peripheral nerve injury and repair. Brain Res. 919(2):302–312; 2001.
71. Valero-Cabre, A.; Navarro, X. Functional impact of axonal misdirection after peripheral nerve injuries followed by graft or tube repair. J. Neurotrauma 19(11):1475–1485; 2002.
72. Valero-Cabre, A.; Tsironis, K.; Skouras, E.; Navarro, X.; Neiss, W. F. Peripheral and spinal motor reorganization after nerve injury and repair. J. Neurotrauma 21(1):95–108; 2004.
73. van Bergeijk, J.; Haastert, K.; Grothe, C.; Claus, P. Valproic acid promotes neurite outgrowth in PC12 cells independent from regulation of the survival of motoneuron protein. Chem. Biol. Drug Des. 67(3):244–247; 2006.
74. Wood, M. D.; Gordon, T.; Kim, H.; Szynkaruk, M.; Phua, P.; Lafontaine, C.; Kemp, S. W.; Shoichet, M. S.; Borschel, G. H. Fibrin gels containing GDNF microspheres increase axonal regeneration after delayed peripheral nerve repair. Regen. Med. 8(1):27–37; 2013.
75. Wood, M. D.; Kim, H.; Bilbily, A.; Kemp, S. W.; Lafontaine, C.; Gordon, T.; Shoichet, M. S.; Borschel, G. H. GDNF released from microspheres enhances nerve regeneration after delayed repair. Muscle Nerve 46(1):122–124; 2012.
76. Wrobel, S.; Serra, S. C.; Ribeiro-Samy, S.; Sousa, N.; Heimann, C.; Barwig, C.; Grothe, C.; Salgado, A. J.; Haastert-Talini, K. In vitro evaluation of cell-seeded chitosan films for peripheral nerve tissue engineering. Tissue Eng. Part A 20(17–18):2339–2349; 2014.
77. Zheng, C.; Zhu, Q.; Liu, X.; Huang, X.; He, C.; Jiang, L.; Quan, D. Improved peripheral nerve regeneration using acellular nerve allografts loaded with platelet-rich plasma. Tissue Eng. Part A 20(23–24):3228–3240; 2014.
78. Zheng, L.; Ao, Q.; Han, H.; Zhang, X.; Gong, Y. Evaluation of the chitosan/glycerol-beta-phosphate disodium salt hydrogel application in peripheral nerve regeneration. Biomed. Mater. 5(3):35003; 2010.
79. Ziv-Polat, O.; Shahar, A.; Levy, I.; Skaat, H.; Neuman, S.; Fregnan, F.; Geuna, S.; Grothe, C.; Haastert-Talini, K. The role of neurotrophic factors conjugated to iron oxide nanoparticles in peripheral nerve regeneration—In vitro studies. Biomed. Res. Int. 2014:267808. doi: 10.1155/2014/267808; 2014.